CHARACTERIZATION OF VWF IN ENDOTHELIAL CELLS

THE CHARACTERIZATION OF VWF IN MOUSE AND HUMAN ENDOTHELIAL CELLS

By ARTHANE KODEESWARAN, B. Sc.

A Thesis Submitted to the School of Graduate Studies in Partial Fulfilment of the Requirements for the Degree Master of Science

McMaster University MASTER OF SCIENCE (2022) Hamilton, Ontario (Medical science)

TITLE: The characterization of VWF in mouse and human endothelial cells

AUTHOR: Arthane Kodeeswaran, B. Sc.

SUPERVISOR: Dr. Davide Matino

PAGES: 72

Lay abstract

Von Willebrand Factor (VWF) is a protein important for blood clotting made in endothelial cells that line blood vessels. VWF is involved in many diseases, particularly unwanted clot formation that leads to arterial and venous thrombosis and may be a good target to treat or prevent such conditions. Gene silencing is an approach that can be used to decrease VWF. Specifically, RNA interference (RNAi) is a type of gene silencing that can be applied using VWF-targeting small interfering RNA (siRNA). When applied, VWF-targeting siRNA will bind to a group of proteins involved in gene silencing called the RNA-induced silencing complex (RISC). The RISC will guide the siRNA to the target VWF mRNA in the cell. Once bound to the target, the target mRNA will be degraded and can no longer be translated into the VWF protein.

To start this process, it is necessary to study the possibility to knockdown (decrease) the VWF in relevant cells, grown in culture plates, before moving to mouse studies. However, there are few studies investigating VWF expression in human and mouse endothelial cells at time points that can be applied to typical gene silencing experiment time points, with no studies investigating VWF expression in mouse cells. This study demonstrates the expression of VWF in one human endothelial cell line and three mouse endothelial cell lines at time points relevant to gene silencing experiments. The results of this study can be used to choose the ideal cell model depending on the experiment and design the experiment based on the VWF expression of the cell line being used.

Abstract

Von Willebrand factor (VWF) is a protein that secreted by endothelial cells and Weibel-Palade bodies of endothelial cells that mediates platelet adhesion and leads to the subsequent clotting at the site of injury. VWF plays a role in hemostatic diseases such as thrombosis. Due to its role in disease, it may be a novel target for the treatment of these diseases. RNA interference (RNAi) is a natural defence mechanism that is being investigated as a therapy for its ability to provide a precise and personalized treatment by silencing specific genes and preventing the translation of target proteins. This makes gene silencing promising for the treatment for many diseases, and VWF knockdown through siRNA could be a potential new strategy for VWF-associated disease. Current methods of *in vitro* study of VWF and ultimately VWD, comprise of the use of VWF-transfected heterologous cells or endothelial cells; however, there are no comprehensive studies investigating the regulation and secretion of VWF over time by endothelial cells, specifically murine endothelial cells that best translate *in vivo* conditions. Any current studies on VWF expression over time are at a shorter time scale that is not compatible with in vitro siRNA transfection protocols. To design siRNA transfection experiments to knockdown VWF in vitro, it is necessary to first investigate VWF expression in human and mouse endothelial cells at time points that can be applied to siRNA transfection. To investigate this aim, several cell lines (HUVEC, LSEC, LMEC and iMAEC) were grown in 24-well plates and treated with PMA, thrombin, or left untreated. RNA, protein lysates and supernatant samples were collected 48 hours post-treatment. Media was changed at 48h and 30-minute, 6h and 24h samples were collected after the media change for analysis through ELISA and qRT-PCR. VWF expression was also visualized in these cells using immunofluorescence. Our findings demonstrate that the expression of VWF in human versus mouse endothelial cells are different, with most similarities demonstrated between HUVECs and LSEC with the expected increase in VWF demonstrated at 48 hours. This data can be used to choose a cell line ideal for future experiments with a longer time scale and/or alter experimental designs depending on the cell line used.

Acknowledgements

I would first like to acknowledge my supervisor Dr. Davide Matino for the continuous support and guidance throughout my time as a graduate researcher. I have learned not only many new laboratory techniques and knowledge on the topics of my project but also how to be a good researcher in general. I would also like to thank my committee, Dr. Colin Kretz, Dr. Peter Gross, and Dr Jeffrey Weitz for all the advice that has shaped this project from the start.

I would like to thank all the members of the Chan/Matino lab for their support. Specifically, Paul Tieu and Helen Atkinson for assistance with any technical aspects of this project, Bonnie Chu for all of her mental support, inspiration and motivation who has truly become one of my best friends inside and outside of this program; and Julia Selmani, my amazing undergraduate student who has learned so much in a short amount of time to help with many aspects of this project.

I would also like to thank my previous supervisors Dr. Byram Bridle and Dr. Brenda Coomber who were the first to lead me to my love for research but also for their continuous advice and support after leaving their labs and becoming a graduate student.

Finally, I would like to thank my parents, sister, and fiancé for their support whether mental, emotional, or financial throughout my time as a graduate student.

Table of contents

Lay abstract……iv

Abstract……v

Acknowledgements……vi

List of figures and tables……x

List of abbreviations……..xii

Declaration of academic achievement……..xiv

Chapter 1: Introduction……1

1.1 Hemostasis……...…..1

1.2 Von Willebrand Factor……..3

1.3 VWF and pathologies……5

1.3.1 Von Willebrand factor and von Willebrand disease……5

1.3.2 Von Willebrand disease and thrombotic thrombocytopenic purpura……..6

1.3.3 Thrombosis……..7

1.3.4 Von Willebrand factor and thrombosis……9

1.4 siRNA……...……...10

1.5 Models used to study VWF……..11

1.6 Hypothesis and objective……15

Chapter 2: Materials and methods……16

2.1 Quantitative characterization of VWF in endothelial cells……16

2.1.1 Endothelial cell culture……16

2.1.1.1 iMAEC……...16

2.1.1.2 HUVEC, LSEC, LMEC……16

2.1.2 Stimulation of endothelial cells……17

2.1.3 Protein analysis……17

2.1.3.1 Protein lysate collection……17

2.1.3.2 ELISA……18

2.1.4 qRT-PCR……..19

2.2 Qualitative characterization of VWF in endothelial cells……22

2.2.1 Endothelial cell culture……22

2.2.2 Stimulation of endothelial cell……..22

2.2.3 Immunofluorescence……22

2.3 Production of a transient mVWF cell line……...23

Chapter 3: Results

3.1 Qualitative VWF expression……24

3.1.1 LSEC……24

3.1.2 LMEC……...27

3.1.3 iMAEC……..29

3.1.4 HUVEC……31

3.2 Fold-change of VWF RNA expression……33

3.2.1 LSEC……33

3.2.2 LMEC……...35

3.2.3 iMAEC……..36

3.2.4 HUVEC……37

3.3 Qualitative VWF expression……38

3.3.1 LSEC……38

3.3.2 LMEC……...42

3.3.3 iMAEC……..46

3.3.4 HUVEC…….50

3.4 HEK293T expressing mVWF……..…54

Chapter 4: Discussion……56

4.1 Limitations and future directions…….59

4.2 Conclusions……..60

Chapter 5: Supplementary Figures…….61

Chapter 6: References……63

List of figures and tables

Figure 1. The coagulation cascade……...2

Figure 2. Domains and functions of VWF……....4

Figure 3. Studies demonstrating VWF expression in HUVEC over time…….14

Figure 4. Experimental design of protein expression experiments……19

Figure 5. Experimental design of RNA expression experiments……...22

Figure 6. mVWF protein expression in untreated LSEC lysates and supernatant over time…….25

Figure 7. mVWF protein expression in untreated and treated LSEC lysates and supernatant over time……26

Figure 8. mVWF protein expression in untreated LMEC lysates and supernatant over time…...27

Figure 9. mVWF protein expression in untreated and treated LMEC lysates and supernatant over time……28

Figure 10. mVWF protein expression in untreated iMAEC lysates and supernatant over time…29

Figure 11. mVWF protein expression in untreated and treated iMAEC lysates and supernatant over time……30

Figure 12. VWF protein expression in untreated HUVEC lysates and supernatant over time…..31

Figure 13. VWF protein expression in untreated and treated HUVC lysates and supernatant over time……32

Figure 14. VWF fold change of treated LSEC……..34

Figure 15. VWF fold change of treated LMEC…….35

Figure 16. VWF fold change of treated iMAEC……36

Figure 17. VWF fold change of treated HUVEC……..37

Figure 18. Untreated LSEC stained with VWF, p-selectin and DAPI……...39

Figure 19. PMA-treated LSEC stained with VWF, p-selectin and DAPI……40

Figure 20. Thrombin-treated LSEC stained with VWF, p-selectin and DAPI……41

Figure 21. Untreated LMEC stained with VWF, p-selectin and DAPI……..43

Figure 22. PMA-treated LMEC stained with VWF, p-selectin and DAPI……..44

Figure 23. Thrombin-treated LMEC stained with VWF, p-selectin and DAPI……...45

Figure 24. Untreated iMAEC stained with VWF, p-selectin and DAPI……47

Figure 25. PMA-treated iMAEC stained with VWF, p-selectin and DAPI……48

Figure 26. Thrombin-treated iMAEC stained with VWF, p-selectin and DAPI…….49

Figure 27. Untreated HUVEC stained with VWF, p-selectin and DAPI……...51

Figure 28. PMA-treated HUVEC stained with VWF, p-selectin and DAPI……52

Figure 29. Thrombin-treated HUVEC stained with VWF, p-selectin and DAPI……53

Figure 30. mVWF and hVWF expression of HUVEC versus mVWF-transfected HEK293T supernatant samples…….55

List of abbreviations

α_2PI	alpha-2 plasmin inhibitor
AGO2-RISC	Argonaute 2-RNA-indiced silencing complex
ADAMTS-13	A thrombospondin type I motif, member 13
BSA	Bovine serum albumin
CTCK	C-terminal cysteine knot
DVT	Deep vein thrombosis
ECM	Extra cellular matrix
ELISA	Enzyme linked immunosorbent assay
ER	Endoplasmic reticulum
FV/Va	Factor V/ activated FV
FVII/FVIIa	Factor VII/ activated FVII
FVIII/FVIIIa	Factor VIII/ activated FVIII
FIX/FIXa	Factor IX/ activated IX
FX.FXa	Factor X/ activated FX
FXI/FXIa	Factor XI/ activated XI
GPIb	Glycoprotein 1 B
HEK293T	Human embryonic kidney cells
HUVEC	Human umbilical vein endothelial cell
IF	Immunofluorescence
iMAEC	Immortalized mouse aortic endothelial cells
LMEC	Lung microvascular endothelial cells
LSEC	Liver sinusoidal endothelial cells

miRNA	Micro RNA
OR	Odds ratio
PAI-1	Plasminogen activator inhibitor 1
PBS	Phosphate buffered saline
PFA	Paraformaldehyde
piRNA	Piwi-interacting RNA
PMA	Phorbol 12-myristate 13-acetate
qRT-PCR	Real time quantitative reverse transcription PCR
RNAi	RNA interference
siRNA	Small interfering RNA
TF	Tissue factor
TTP	Thrombotic thrombocytopenic purpura
VTE	Venous thromboembolism
VWD	Von Willebrand Disease
VWF	Von Willebrand factor
WPB	Weibel-Palade body

Declaration of academic achievement

I, Arthane Kodeeswaran, declare the work of my thesis to be my own. I am the sole author of this document. While I am the primary contributor to this project, this research was performed with the assistance of Julia Selmani of McMaster University at TaARI and designed with the assistance of Dr. Davide Matino. This project was financially supported by Dr. Davide Matino.

Chapter 1: Introduction

1.1 Hemostasis

Hemostasis is a physiological response that reduces blood flow and initiates blood clotting at the site of vascular injury to prevent blood loss (Turpie & Esmon, 2011). Normal hemostatic response to vascular injury includes blood vessel restriction to decrease blood flow, platelet adhesion, activation and aggregation, and blood coagulation (Turpie & Esmon, 2011). This leads to the formation of a platelet plug to reduce blood loss. At the beginning stages of hemostasis, endothelial injury constricts the blood vessel to reduce blood flow and exposes the collagen of the blood vessel. Platelets bind to the collagen leading to platelet activation and aggregation (Monroe & Hoffman, 2006). This is the formation of the primary platelet plug to temporarily prevent blood loss (Davie *et al.*, 1991). Vascular injury also exposes tissue factor (TF). The exposure of the subendothelial TF activates the coagulation cascade, ultimately leading to fibrin formation and the final hemostatic plug (Furie & Furie, 2008).

The coagulation cascade is comprised of the initiation phase, amplification phase, propagation phase, and clot formation, as illustrated in figure 1. The initiation phase begins with the activation of TF. TF binds to factor VIIa (FVIIa) to form the TF-FVIIa complex that leads to a cascade of factor activation, starting with the activation of factor X (FX) to FXa. FXa activates factor V (FV), after which FXa and FVa combine to form prothrombinase. This results in the conversion of prothrombin to thrombin in the presence of a negatively charged surface (Monroe & Hoffman, 2006). During the amplification phase, aside from activating platelets, thrombin also activates FV and factor VIII (FVIII), which then amplifies thrombin generation to increase both

thrombin generation and platelet activation (Monroe & Hoffman, 2006). Thrombin also activates platelet-bound factor XI (FXI) during the amplification phase (Turpie & Esmon, 2011).

During the propagation phase, platelets are recruited to the site of injury. FXIa on the surface of the platelets activates factor IXa (FIXa) which then forms a complex with FVIIIa to activate FX. FXa again forms a complex with FVa to generate more thrombin (Palta *et al.*, 2014). The newly generated thrombin cleaves soluble fibrinogen into insoluble fibrin, creating the fibrin clot (Adams & Bird, 2009).

Finally, the clot will be resolved through fibrinolysis. Outside of the clot, the serpins plasminogen activator inhibitor 1 (PAI-1) and alpha-2 plasmin inhibitor (α_2PI) will inhibit both plasmin and plasmin activator, ultimately inhibiting fibrin formation (Longstaff and Kolev, 2015).

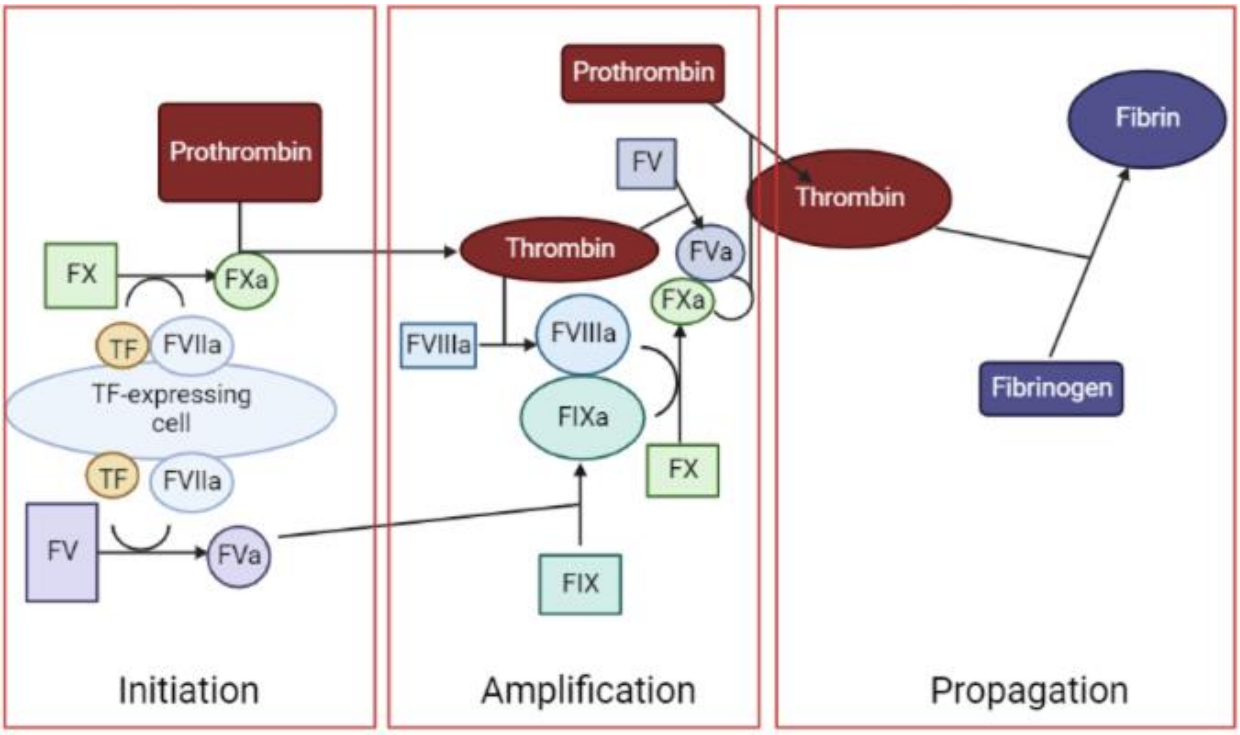

Figure 1. The coagulation cascade. Adapted from: Turpie & Esmon, 2011.

1.2 Von Willebrand Factor

von Willebrand factor (VWF) is a large multimeric glycoprotein critical for hemostasis. VWF is produced by endothelial cells and megakaryocytes as a prepropolypeptide (Lenting *et al*., 2012). As demonstrated in figure 2, the primary structure of VWF contains multiple repeating domains, each with different structures and functions (Lenting *et al*., 2012). VWF monomers dimerize through the C-terminal cysteine knot (CTCK) domain through disulfide bonds in the endoplasmic reticulum (ER) and travel to the *trans*-Golgi. Here, the D1D2 fragments will dimerize, and CTCK to A2 domains will form "dimeric bouquets" (Zhou *et al*., 2012; Springer, 2014). In the Golgi apparatus, pro-VWF is cleaved and starts forming tubules that are packed in Weibel-Palade bodies (WPB) as multimers of varying sizes (Nightingale and Cutler, 2013). VWF is stored and secreted from the WPB of endothelial cells and α-granules of platelets (Lenting *et al*., 2012).

Tubule formation of VWF drives the initial formation of WPB in the *trans*-Golgi network (Nightingale and Cutler, 2013). Once released from the *trans*-Golgi network, WPB are distributed to the periphery of endothelial cells where VWF, P-selectin and other proteins contained in WPB can be released (Nightingale and Cutler, 2013). α-granules of platelets release VWF in response to platelet activation; however, VWF release from WPB may be both constitutive and regulated, with constitutive secretion being the most accepted (Lenting *et al*., 2012). WPB move throughout the cytoplasm with no stimulation, undirected until a WPB moves to the periphery of the endothelial cell (Lenting *et al*., 2012). Then, the WPB fuses with the plasma membrane, releasing VWF into the blood or subendothelium (Babich *et al*., 2008). While this is unregulated, in certain instances, a rise in pH of the WPB from exposure to the

extracellular environment can result in VWF tubules deforming, preventing secretion (Babich *et al*., 2008).

Once secreted, large VWF multimers are cleaved by a disintegrin and metalloproteinase with a thrombospondin type I motif, member 13 (ADAMTS13), a metalloprotease, through the unfolded A2 domain (Hassan *et al.*, 2012). This results in smaller, less prothrombotic multimers (Hassan *et al.*, 2012). VWF binds platelet receptor glycoprotein Ib (GP1b) with strong affinity through the A1 domain (Hassan *et al.*, 2012). This contributes to one of the main roles of VWF, mediating platelet activation, adhesion, and aggregation, which is essential for thrombus formation (Hassan *et al.*, 2012). Through the A1 and A3 domains, VWF binds to collagen (Hassan *et al.*, 2012). When VWF binds the injured endothelium through collagen, it also binds to GPIb, allowing for platelet tethering to the vessel wall at high shear rates (Hassan *et al.*, 2012). Through the D' and D3 domains, VWF binds FVIII, protecting it from degradation while prolonging its half-life and transporting it to the site of injury (Springer, 2014). VWF is sent for clearance mainly through an active regulatory mechanism and is targeted to the liver and spleen (Lenting *et al*., 2012). There is evidence that indicates that VWF is endocytosed by macrophages through receptor-mediated endocytosis (Lenting *et al*., 2012).

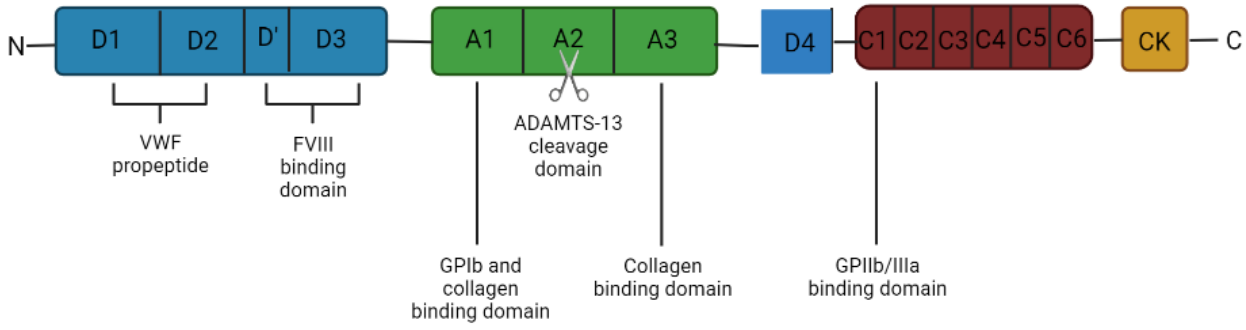

Figure 2. Domains and functions of VWF. Adapted from: Crawley and Scully, 2013.

1.3 VWF and pathologies

Pathological coagulation occurs when the equilibrium of blood clot formation and resolution is disrupted (Harter *et al*., 2015). When this balance is disrupted towards a pro-coagulant state, clots can form and block arteries and veins (thrombosis) and travel to other, larger vessels (embolism). The blockage of these vessels can lead to severe complications such as pulmonary embolism and stroke (Kim *et al*., 2017). An imbalance of the opposite side of the spectrum can lead to bleeding disorders. This includes inherited bleeding disorders such Von Willebrand disease (VWD), caused by a decrease or dysfunction of VWF (Campioni *et al.*, 2021; Hurwitz *et al.*, 2017). VWF plays a key role in disorders of both imbalances including thrombosis and VWD.

1.3.1 Von Willebrand factor and Von Willebrand disease

VWD is an inherited bleeding disorder characterized by a decrease or dysfunction in VWF (Peyvandi *et al.*, 2019). VWD is a highly heterogenous, autosomally inherited disease caused by genetic mutations that lead to a qualitative or quantitative defect in VWF. This can be categorized as type I, II, and III (Nichols *et al.*, 2008). In turn, this results in abnormalities in platelet adhesion and aggregation as well as changes in FVIII levels, and ultimately the coagulation cascade and clotting (Nichols *et al.*, 2008).

Type I VWD, or partial-quantitative VWD is characterized by a partial reduction in VWF and presents mild bleeding symptoms; however, in some cases, changes in clotting may not be apparent (Goodeve *et al.*, 2007). Type II VWD, or qualitative VWD is characterized by changes in VWF function, and can be further categorized into A, B, M and N subtypes (Hassan *et al.*, 2012). Type IIA VWD is caused by VWF that is dysfunctional, although they may be in normal

circulating levels (DiGiandomenico *et al.*, 2020). Type IIB VWD is characterized by platelets binding VWF in circulation instead of at the site of injury. Type IIM and IIN VWD is characterized by reduced binding of VWF to GPIb and FVIII respectively (DiGiandomenico *et al.*, 2020). Type III VWD, the most severe form, is characterized by a near complete depletion of VWF; varying in severity and symptoms and may present as bleeding including epistaxis, cutaneous bleeding, and hemarthrosis (Christopherson *et al.*, 2022).

All three types of VWD are a result of a decrease in the amount of VWF or a decrease in the amount of functional VWF. Overall, this results in altered platelet function and FVIII levels, leading to a bleeding phenotype.

Current treatments for VWD include Desmopressin or VWF/FVIII replacement therapy to increase plasma VWF and FVIII (Castaman *et al.*, 2013). However, frequent administration is required and not all patients respond equally to these treatments (Castaman *et al.*, 2013).

1.3.2 Von Willebrand Factor and Thrombotic Thrombocytopenic purpura

Thrombotic thrombocytopenic purpura (TTP) is a disease characterized by a deficiency in ADAMTS-13. As large VWF multimers are cleaved by ADAMTS-13, this deficiency can also result in the accumulation of ultra large VWF multimers (Sukumar *et al.*, 2021). The accumulation of ultra large VWF multimers can in turn lead to spontaneous platelet adhesion and aggression and ultimately disseminated microthrombi (Sukumar *et al.*, 2021).

A study by de Maat *et al* investigated a fusion protein, “Microlyse,” that targets VWF-platelet complexes for destruction (2022). de Maat *et al* discovered that the administration of Microlyse into a TTP mouse model degraded microthrombi and reduced thrombocytopenia (2022). A study by Jilma-Stohlawatez *et al.* demonstrated that a VWF-inhibiting aptamer

stabilized platelet counts in patients with TTP, further demonstrating the role of VWF in TTP. (2011)

1.3.3 Thrombosis

Thrombosis is the pathologic formation of a blood clot or thrombus in a blood vessel (Oklu, 2017). Thrombi can eventually break off and turn into emboli, which in turn can block major blood vessels, leading to other pathologies (Kleinschnitz *et al*., 2009). The two types of thrombosis include arterial thrombosis and venous thrombosis, which are treated as two different pathologies due to their distinct characteristics (Turpie & Esmon, 2011).

Arterial thrombosis is triggered by the rupture of atherosclerotic plaques (Jackson, 2011). Arterial plaques consist of cholesterol, lipid deposits and macrophages (Mackman, 2008). The rupture of the plaque leads to the lipid core of the plaque, containing TF, to be exposed to the blood. The exposure of the TF and collagen present in the plaque lead to platelet recruitment, aggregation, and adhesion, ultimately resulting in thrombus formation (Westein *et al.*, 2013). TF also activates the coagulation cascade, amplifying thrombin and fibrin formation and platelet activation/adhesion, contributing to the growth of a platelet-rich thrombus (Papageorgiou *et al*, 2013). The fibrin network of the thrombus traps red blood cells in the final stages of thrombosis (Lipinski *et al*, 2012).

Inflammation also contributes to atherosclerosis and arterial thrombosis (Moriya, 2019). During the initial phases of atherosclerosis, an atheroma is formed. A few of the main constituents of an atheroma include inflammatory and immune cells. Once activated, these immune cells produce inflammatory cytokines and proteases that destabilize the plaque, resulting in rupture (Moriya, 2019).

Venous thrombosis results of imbalances of Virchow's triad that consists of blood stasis, vascular injury, and hypercoagulability of blood (Wolberg *et al.*, 2012). Stasis, or the reduction of blood flow, can occur from immobility and increased venous pressure (López & Chen, 2009). This results in a slower blood flow, leading to a slower clearance rate of circulating coagulation factors at the site of injury (Turpie & Esmon, 2011). Vascular injury results in the exposure of subendothelial TF, leading to platelet adhesion and the activation of the coagulation cascade; this results in the production of fibrin (Turpie & Esmon, 2011). Hypercoagulability of blood refers to a state where the blood is more prone to clotting. This is due to the increase of clotting proteins, decrease of anticoagulant proteins, and a decrease in fibrinolysis (Mackman, 2008). The increase of clotting proteins of the hypercoagulation of blood, exposure of TF from vascular injury, and slow clearance of coagulation factors from reduced flow all contribute to the unbalanced increase of the coagulation cascade, resulting in fibrin formation and buildup, and thrombus formation (Mackman, 2008).

Both venous and arterial thrombosis can result in serious complications, however, the results vary depending on the type. Arterial plaques resulting in thrombosis can lead to unstable angina and acute myocardial infarctions (Newby *et al.*, 2011). In patients with atrial fibrillation, thrombi often form in the left atrium. Thrombi in patients with atrial fibrillation increase the risk of ischemic stroke (Nieswandt & Bender, 2011). When venous thrombi break of the vessel wall, they can travel to the lungs, resulting in a pulmonary embolism, blocking blood flow to the lungs (Mackman, 2008).

Conventional treatments thrombosis such as traditional anticoagulants and direct oral anticoagulants, and antiplatelet therapies may have adverse and unpredictable pharmacokinetic responses and side effects including severe bleeding (Kim *et al.*, 2017).

1.3.4 Von Willebrand factor and thrombosis

VWF has been demonstrated to play a role in venous thrombosis. In a study by Brill *et al.* a flow restriction mouse model was used to demonstrate the role of VWF in deep vein thrombosis (DVT) (2011). After a complete blood flow stasis in VWF deficient mice, the prevalence of thrombus formation as well as the size and weight of the thrombus was reduced compared to wildtype mice (Brill *et al.,* 2011). In the stenosis model VWF deficient mice were completely protected from thrombus formation (Brill *et al.,* 2011). A study by Edvardsen *et al.* (2021) demonstrated that high plasma VWF in humans are associated with an increased risk of developing venous thromboembolism (VTE). Blood from participants with VTE and age/sex matched controls was collected, and the odd ratio (OR) was estimated across quartiles corresponding with increasing VWF levels (Edvardsen *et al.* 2011). Participants were followed until incidence of VTE, death, or end-of-study follow- up (Edvardsen *et al.* 2011). Based on this study, the risk for developing VTE increased with increasing levels of VWF (Edvardsen *et al.* 2011).

VWF has also been demonstrated to play a role in arterial thrombosis. A study by Kleinschnitz *et al.* demonstrated that VWF deficient mice were protected (2009) from ischemic stroke (Kleinschnitz *et al.*, 2009). In this study, middle cerebral artery occlusion was induced in VWF-deficient and wildtype mice (Kleinschnitz *et al.,* 2009). Compared to controls, VWF-deficient mice had smaller infarctions by about 60% after 24 hours and demonstrated better neurological function (Kleinschnitz *et al.*, 2009). A study by Sanders *et al.* investigated the association between VWF deficiency and the prevalence of arterial thrombosis (2013). The prevalence of arterial thrombosis in VWF-deficient patients was observed and they found that the prevalence of all arterial thrombotic events in VWF-

deficient patients was 39% and 63% lower than the two reference populations (Sanders *et al.,* 2013).

The role of VWF in thrombosis and VWD suggest that targeting VWF may be a viable option for the treatment of these disorders.

1.4 siRNA

A possible avenue to modulate VWF secretion is RNA interference (RNAi). RNAi is a naturally occurring, biological process that regulates gene expression (Chery, 2016). Different types of RNAi include the use of piwi-interacting RNA (piRNA), microRNA (miRNA) and small-interfering RNA (siRNA) (Chery, 2016). Double stranded siRNA that corresponds with the RNA of the target protein will enter the cell where it binds the Argonaute 2-RNA-induced silencing complex (AGO2-RISC complex) (Chery, 2016). Once bound to the activated RISC, the siRNA will separate into sense and antisense strands (Chery, 2016). The antisense strand will guide the activated RISC to the target, complementary mRNA (Chery, 2016). The antisense strand with the RISC will bind the target mRNA, allowing AGO2 to cleave the mRNA, triggering degradation by exonucleases and preventing protein translation (Chery, 2016).

The use of siRNA and other oligonucleotides comes with barriers. One of the main barriers includes the siRNA's susceptibility to degradation by nucleases, which can result in a decreased ability to knockdown the target protein (Kher *et al.,* 2011). Another barrier is the cell uptake of the siRNA; siRNA delivered naked, is not cell specific and can result in less siRNA being taken up by target cells which may result in non-target cells taking up siRNA, leading to off-target effects (Kher *et al.,* 2011). Due to the larger molecular mass and negative charge compared to other oligonucleotides, it may be more difficult enter the cell through the cell

membrane (Kher *et al.,* 2011). To overcome these barriers, various vectors and modifications are being studied as possible solutions.

A common strategy currently being studied are lipid-based delivery systems. Since cell membranes are composed of lipid bilayers, lipid-based delivery may aid in carrying the siRNA across the cell membrane. Lipid-based vectors such as lipid nanoparticles (LNP) enter the cell through endocytosis do to the similar composition to the cell membrane (Schroeder *et al.,* 2010). Once internalized to the cell, the endosome will acidify, causing amine groups that are a part of the vector to be protonated. This leads to the subsequent influx of protons and chloride ions, leading to an osmotic imbalance (Schroeder *et al.,* 2010). The result of this imbalance is water entering and inflating the endosome, causing the rupture and release of siRNA into the cytoplasm (Schroeder *et al.,* 2010). Cholesterol-conjugation is a method where cholesterol will bind circulating plasma lipoproteins which will interact with lipoprotein receptors to allow the siRNA to enter the cell (Osborn and Khvorova, 2018). *In vitro,* cholesterol-conjugation has been demonstrated to exhibit rapid internalization by any cell type through EEA1-associated endocytosis. The cholesterol-conjugated siRNA showed accumulation in extra-hepatic tissues including muscle and lung tissue after a single subcutaneous injection Osborn and Khvorova, 2018).

1.5 Models used to study VWF

While the distribution of VWF in tissues has been studied, there are limited studies investigating the *in vitro* expression VWF, with most studies examining human endothelial cells (Pan *et al*., 2016; Yamamoto *et al.,* 1998). Comprehensive studies on the expression of VWF in mouse endothelial cells can provide insight into VWF expression that may be better applied to

design *in vivo* mouse studies. Aside from *in vivo* studies, human umbilical vein endothelial cells (HUVEC) are predominantly used to study VWF, however, studies have not demonstrated whether HUVEC expression of VWF is comparable to endothelial cells of other species (Lenting *et al*., 2012). Another method of study consists of the use of VWF-transfected heterologous cells; however, this does not mimic the endothelial environment (Lenting *et al*., 2012). Investigating the secretion of VWF in HUVECs versus mouse endothelial cells may provide more insight into the expression of VWF and more *in vitro* models to study VWF which could be applied to the study of VWF and disease.

Specifically, there is a gap in literature examining the expression of VWF *in vitro* in the context of long-term experiments such as siRNA transfection. Typically, when transfecting cells with siRNA *in vitro*, the experiments are performed on the scale of days (Kamalzare *et al.*, 2019; Takahashi *et al*, 2015; Hwang *et al*, 2010). Transfected cells are incubated for 24 hours to 72 hours for optimal knockdown (Kamalzare *et al.*, 2019; Takahashi *et al*, 2015; Hwang *et al*, 2010). When comparing this to our current knowledge of VWF expression in endothelial cells, studies have only been performed in HUVECs, ad at shorter time-points. These studies were performed up to 24 hours in the scale of minutes to hours, but not at time points that correlate with siRNA transfection in the scale of days as demonstrated in figure 3 (Turner *et al.*, 2009; Meiring *et al.*, 2016).

Specifically, we want to investigate the use of cholesterol-conjugated siRNA to target VWF. Using our protocol developed from the suggestion of Advirna (company manufacturing conjugated siRNA), we plan to treat cells with 100uM of conjugated siRNA at 30% confluency. We will change media after 48 hours of incubation to remove any residual siRNA and collect samples 24 hours after that. Since residual VWF was removed, we hypothesize that the

subsequent secretion of VWF in siRNA treated groups will be lower than untreated. Like the siRNA transfections performed in the papers above, this transfection happens over a longer period of time, with the experiment running for 72 hours with a media change at 48 hours. This means we require cell lines that produce sufficient VWF at these time points and insight into the expression pattern of VWF without VWF knockdown at these time points.

As mentioned, HUVECs are predominantly used for many VWF-related studies; however, there are no studies evaluating VWF expression in HUVECS over a larger time scale. There are also no studies investigating VWF expression in mouse endothelial cells. Studies examining and comparing VWF expression in HUVECs and mouse endothelial over days can provide insight into the mouse cell line that is most comparable to HUVECs in VWF expression, and the ideal timepoints and experimental design for VWF knockdown using siRNA.

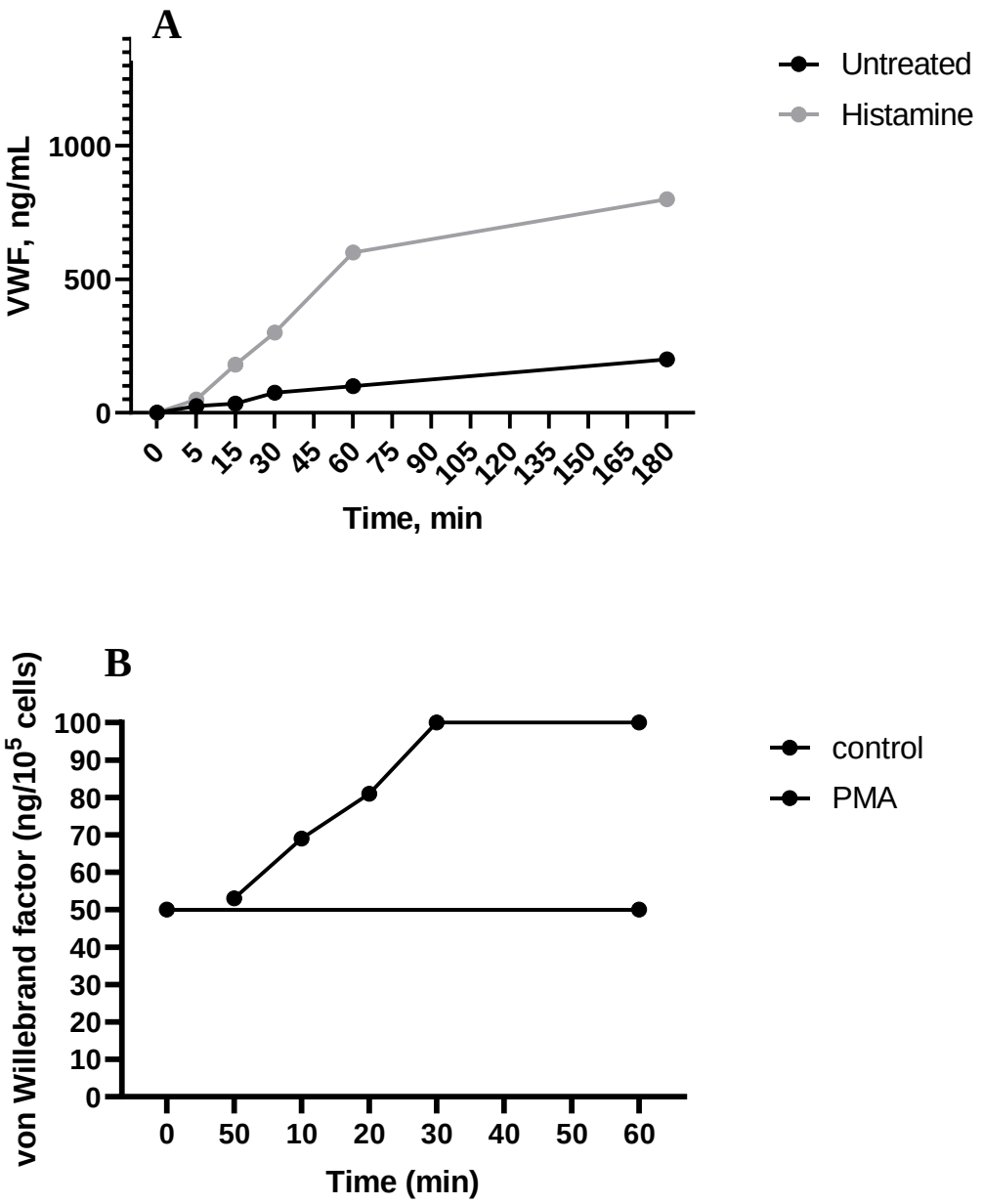

Figure 3. Studies demonstrating VWF expression in HUVEC over time at 0 minutes to 180 minutes unstimulated vs histamine treated (A) and 0 to 60 minutes, unstimulated vs PMA-treated (B) (Adapted from: Turner *et al.*, 2009; Meiring *et al.*, 2016).

1.6 Hypothesis and objective

The aim of this study is to characterize basal and regulated secretion of VWF *in vitro* in human and mouse endothelial cells at a time scale relevant to siRNA transfection. We expect to see an increase in VWF secretion over time. When stimulated with secretagogues, we hypothesize that there will be an increase in VWF secretion compared to untreated cells. We expect to see this both quantitatively and qualitatively. Investigation of the expression of VWF in mouse endothelial cells may provide insight into optimal models and study design for *in vitro* VWF studies, specifically for experiments with longer incubations such as siRNA transfection. This study can also provide insight into *in vitro* models that best translate into *in vivo* mouse conditions to study VWF-associated disease.

Chapter 2: Materials and methods

2.1 Quantitative characterization of VWF in endothelial cells

2.1.1 Endothelial cell culture

2.1.1.1 immortalized mouse aortic endothelial cells

Immortalized mouse aortic endothelial cells purchased from ABM were cultured on Pricoat extracellular matrix (ECM) pre-coated T25 flasks (ABM) in 7mL Prigrow III media (ABM) with supplements (10% FBS-ABM, 1% penicillin/streptomycin-ABM, 1X non-essential amino acids-ABM, 50ug/mL ECGS-corning). Once cells reach 70% confluency, they were split into 24-well plates coated with ECM at 20 000 cells/cm^2 in 600uL media. Culture plate was prepared by coating each well with 200uL ECM for 1 hour in the biosafety cabinet, aspirating contents, and drying for 1 hour.

2.1.1.2 human umbilical vein endothelial cells, mouse liver sinusoidal endothelial cells, mouse lung microvascular endothelial cells

HUVECs purchased from Lonza were previously passaged and stored at P3 generations. P3 HUVEC was cultured in 10 mL EGM-2 complete media on a 2% gelatin coated, 10cm cell culture plate. At 70-80% confluency, cells were split into 24-well plates at 40 000 cells/cm^2 in 600uL media.

The protocol described above was followed exactly for culturing mouse liver sinusoidal endothelial cells (mLSEC) and mouse lung microvascular endothelial cells (mLMEC) with Endothelial cell complete media (Cell biologics).

2.1.2 Stimulation of endothelial cells

Cells were P4 at the time of treatment. Once cells in the 24-well plates were 30% confluent (to mimic siRNA treatment conditions), cell supernatant and protein lysates were collected and they were treated as three groups: untreated control, 100ng/mL phorbol 12-myristate 13-acetate (PMA; Sigma), and 2IU/mL thrombin (mouse: Oxford biomedical, human: Enzyme research laboratories). After 48-hours, the samples for the same groups as above were collected. Remaining cells were then washed with PBS and fresh media was added. Supernatant, and protein lysates were then collected for 30 minute, 6-hour, and 24-hour timepoints after the media change. The 48 hour and 30 minutes time points were chosen to ensure that residual VWF was removed, to mimic the siRNA experimental design. The 6 hour and 24-hour time points were chosen to ensure that there is an increase in VWF at the time that samples would be collected for siRNA transfection. Separate wells were used for each replicate of each time point. The experimental design is shown in figure 4.

2.1.3 Protein analysis

2.1.3.1 protein lysate collection and quantification

To collect protein lysates, wells were washed twice with 500uL 1X PBS. 200uL 0.5% trypsin-EDTA (Gibco) was added to cells and incubated at 37°C until cells were detached. Once detached, 300uL of the appropriate cell culture media was added to stop reaction and cells were transferred into 1.7 mL microtubes. Cells were centrifuged 500xG for 5 minutes at room temperature and supernatant was discarded. The cell pellets were then resuspended in 500uL cold PBS and spun at 500xG for 5 minutes at 4°C. Supernatant was discarded and the pellet was resuspended in 100uL complete RIPA lysis buffer. RIPA buffer was prepared with 5M NaCl (Bioshop), 0.5M EDTA (BDH), 1M Tris (Bioshop), Triton X-100 (Biorad), 10% sodium

deoxycholate (BBL), 10% SDS (Bioshop), 10mM NaF (EM Science) and topped up with milliQ water. Right before use, 100mM PMSF (Sigma) and 1X complete protease inhibitor tablets (Roche) were added to 1mL RIPA to make complete RIPA buffer. Cell pellets resuspended in RIPA buffer were immediately vortexed for 5 seconds and incubated on ice for 15 minutes. Then, lysates were sonicated 3 times, 2 seconds each with a 1-minute rest between rounds. Samples were then incubated on ice for 15 minutes. Finally, cells were spun at 13 000xG for 5 minutes at 4°C and the supernatant was transferred to a new tube.

The Pierce BCA protein assay kit (Thermofisher) was used to quantify the total amount of protein in each lysate sample. Samples and BSA standards (20-2000ug/mL) were loaded onto a 96 well plate. 200uL BCA working reagent was added to each well and incubated for 30 minutes at 37°C for 30 minutes. Absorbance was measured at 562 nm and the standard curve was used to interpolate total protein concentrations.

2.1.3.2 ELISA

Human VWF ELISA:

Human VWF match paired antibodies (Affinity Biologicals) was used with Normal Control Calibrator Plasma (Affinity biologicals) and the Visulize Buffer Pak (Affinity biologicals) was used to quantify VWF expression in HUVEC. 100uL of samples and standards (0-139 ng/mL) were plated on plates previously incubated with capture antibody and blocking buffer. Samples were incubated for 90 minutes and washed off before adding 100uL detector antibody per well. After incubating for 90 minutes, OPD Substrate was added, and reaction was stopped with 2.5M H_2SO_4. Absorbance was measured at 490nm and total protein measured through BCA was used to normalize results.

Mouse VWF ELISA:

Mouse VWF A2 match paired antibody and standards (Abcam) were used with the ELISA accessory pack (Abcam) to quantify VWF expression in mouse endothelial cells. After incubating with 2ug/mL capture antibody and blocking the plate, 50uL samples and standards (0-4000pg/mL) were added per well and incubated for 2 hours. After washing plates, 0.5ug/mL detector antibody was added per well and incubated for 1 hour. Then, plate was washed and 0.05ug/mL Streptavidin-HRP was added and incubated for 1h. After plate was washed, 100uL TMB Substrate was added. Once optimal colour developed, 100uL stop solution was added and the endpoint was measured at 450nm total protein measured through BCA was used to normalize results.

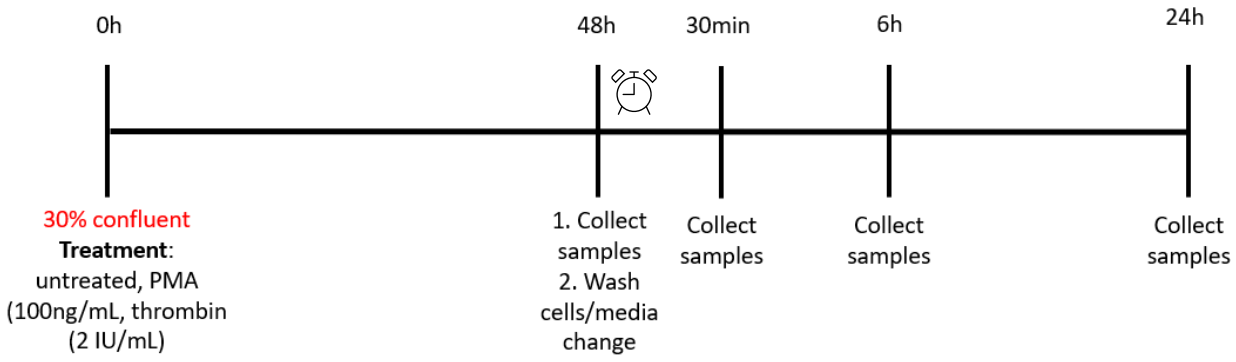

Figure 4. Experimental design: HUVEC, LSEC, LMEC and iMAEC were treated with PMA and thrombin or left untreated at 30% confluency. Samples were collected at 0h, 48h, 30min, 6h, 24h

2.1.4 qRT-PCR

All cells were plated and treated as described above. Samples were collected 48 hours after treatment, and 30 minutes, 6 hours and 24 hours after the 48-hour media change, as shown in figure 5. RNeasy mini kit (Qiagen) and QIAshredder (Qiagen) were used to prepare RNA lysates, and extract and purify RNA.

Cells were harvested by aspirating cell culture media and adding 350uL of buffer RLT. A micropipette was used to mix and add harvested cells into a QIAshredder spin column to

homogenize the samples. In the spin column, cells were spun at full speed for 2 minutes. Then, 300uL of 70% ethanol was added to samples, mixed, and transferred into the RNeasy spin column and collection tube. The samples were spun at 10 000xG for 15 seconds at room temperature. Flowthrough was discarded and 700uL of buffer RW1 was added to spin column and spun at 10 000xG for 15 seconds. Flowthrough was discarded and 500uL buffer RPE was added to the spin column and spun at 10 000xG for 15 seconds. Spin column was then placed in a new tube and spun at full speed for 1 minute to remove any residual flow through and place in another new tube. 25uL RNAse-free water was added to spin column and spun at 10 000xG for 1 minute to elute RNA. RNA yield and purity was quantified using a NanoDrop. spectrophotometer.

A high-capacity cDNA reverse transcription kit (Applied biosystems) was used to reverse transcribe RNA into cDNA. 10uL of 250ng RNA was added to 10uL RT master mix from kit containing 10X RT Buffer, 25X dNTP mix, 10X RT random primers, MultiScribe Reverse™ Transcriptase, RNase Inhibitor, and nuclease free water into PCR reaction tubes (Biostore). Tubes were briefly centrifuged and loaded on the thermocycler (BioRad) with the following conditions as a 20uL reaction:

1. 25°C for 10 minutes
2. 37°C for 120 minutes
3. 85°C for five minutes
4. 4°C infinite hold

qPCR was then run using the cDNA obtained and the Power SYBR green RT-PCR Master mix (Applied biosystems) in a 25uL reaction with the following primers:

B-actin housekeeping primers

mouse F: GGGGTGTTGAAGGTCTCAAAC

R: GGCACCACACCTTCTACAATG

human F: ACCGAGCGCGGCTACAG

R: CTTAATGTGACGCACGATTTC

VWF test primers

mouse: F: GCAGTGGAGAACAGTGGTG

R: GTGGCAGCGGGCAAAC

human: F: TAAGAGGGCAACACAAACG

R: ATCTTCACCTGCCCACTCC

Samples were run at the following conditions: 95°C for 10 minutes, and 40 cycles of 95°C for 15 seconds and 60°C for 60 seconds. The fold change between treated and untreated samples were calculated using the following formula:

Fold change = $2^{-\Delta\Delta Ct}$, where $\Delta\Delta Ct = \Delta Ct$ (treated) – ΔCt (untreated) and ΔCt = Ct (VWF gene) – Ct (housekeeping gene/B-actin)

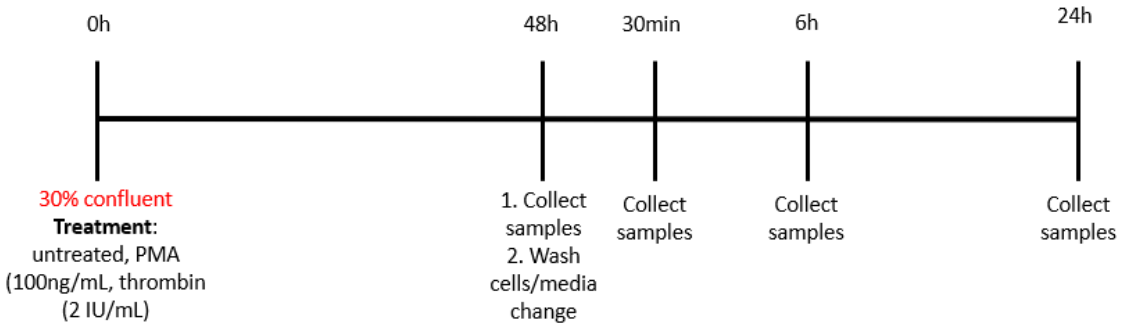

Figure 5. Experimental design: HUVEC, LSEC, LMEC and iMAEC were treated with PMA and thrombin or left untreated at 30% confluency. Samples were collected at 0h, 48h, 30min, 6h, 24h

2.2 Qualitative characterization of VWF in endothelial cells

2.2.1 Endothelial cell culture

Cells were cultured as described above. Cells were then split into ECM-coated or gelatin-coated round glass coverslips in 24-well plates.

2.2.2 Stimulation of endothelial cells

Once cells reached 50% confluency, they were treated as described above. Cells were treated at 50% confluency to ensure they were 70-80% confluent at the time of sample collection for optimal visualization during immunofluorescence.

2.2.3 Immunofluorescence

24 hours after treatment, cells were fixed with 4% paraformaldehyde (PFA) (Fisherbrand) in PBS and blocked in 5% BSA (Sigma), 0.25% Triton X-100 in PBS. Triton X-100 was added to blocking buffer to allow for permeabilization. Cells were incubated with P-selectin (also stored in Weibel-Palade bodies) and VWF primary antibodies (Affinity biologics goat anti-human VWF: 1:200; Invitrogen mouse anti-human p-selectin: 1:100; Invitrogen rabbit anti-

mouse VWF: 1:100; R&D systems goat anti-mouse p-selectin: 1:40). Cells were then incubated with secondary antibodies (Invitrogen chicken anti-goat-Alexa fluor 488 1:500; Invitrogen goat anti-mouse-Alexa fluor 568 1:1000; Invitrogen donkey anti-rabbit-Alexa fluor 568 1:500) and stained with 1ug/mL DAPI. Stained coverslips were mounted onto glass slides and sealed. Slides were imaged using confocal microscopy (Leica Stellaris) at 20X and 63X objectives within one week of staining

2.3 Production of a transient mVWF cell line

VWF DNA in a pcDNA 3.1 vector (Biobasics) was incubated with E. coli cells in LB medium (Bioshop) and heat shocked. Cells were cultured overnight. Maxiprep kit (Qiagen) was used to obtain mVWF DNA pellet from E. coli cells containing the mVWF pcDNA plasmid.

20ug of VWF DNA was transfected using lipofectamine 3000 and Opti-MEM (Invitrogen) in human embryonic kidney (HEK293T) cells grown in DMEM, 10% FBS, 1% penicillin/streptomycin. Once 80% confluent, cells were split in selection media (DMEM, 10% FBS, 1% penicillin/streptomycin, 0.1mg/mL G418) to select colonies. Once colonies were visible, colony selection discs were used to transfer individual colonies to 48-well dishes. Once each well was confluent, supernatant was collected and analysed by mVWF ELISA as described above and top two colonies producing VWF “HEK 293-O” and HEK 293-Q” were expanded and frozen.

HUVEC and HEK 293-O supernatant samples were both run on human and mouse VWF ELISAs as described above.

Chapter 3: Results

This study investigated VWF expression and secretion over time in mouse and human endothelial cells through quantitative and qualitative measures.

3.1 Quantitative VWF protein expression

After culturing LSEC, LMEC, iMAEC and HUVEC, for 48h after cells were 30% confluent, cells were washed, and media was replaced with fresh media to remove residual VWF. 48-hour time point supernatant, and protein lysate samples were collected immediately before changing media. After changing media, the same samples were collected at 30-minute, 6-hour, and 24-hour timepoints.

Next, LSEC, LMEC, iMAEC and HUVEC, were treated with PMA and thrombin at 30% confluency. 48 hours after cells were treated, cells were washed, and media was replaced with fresh media. 48-hour time point supernatant, and protein lysate samples were collected immediately before changing media. After changing media, the same samples were collected at 30-minute, 6-hour, and 24-hour timepoints. A summary table comparing expression can be found in the appendix (Table S1).

3.1.1 LSEC

Figure 6a demonstrates an overall increase in mVWF in LSEC from 0h to 24h for supernatant samples. There is also a slight decrease seen after the media change seen at 30 minutes in the supernatant. Figure 6b demonstrates a similar mVWF level in the lysates for all timepoint until the increase seen at 24 hours. As expected, the overall increase at 24 hours corresponds with the increase seen at 24 hours in the lysates.

Figure 7 demonstrates there was no increase in mVWF in the lysates or supernatant of PMA or thrombin treated cells versus untreated control in the LSEC.

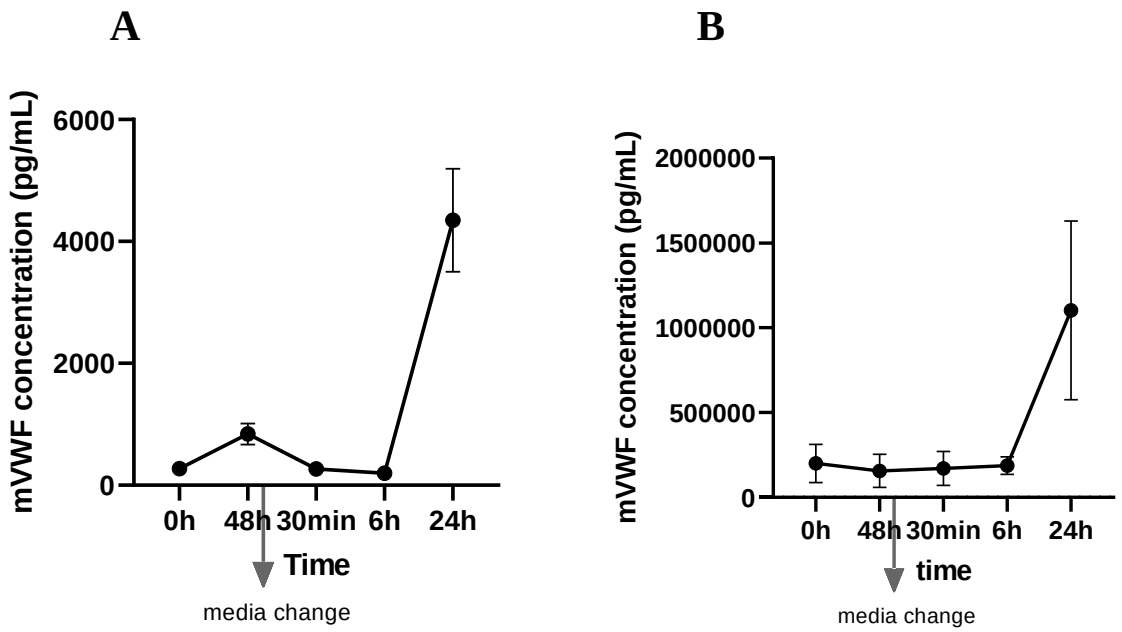

Figure 6. Untreated LSEC were grown to 30% confluency (0h) and samples were collected. Samples were then collected 48h later, and media was replaced. 30 minutes, 6h and 24h after media was changed, supernatant and lysate samples were collected, and ELISA was performed. This figure demonstrates mVWF concentration of untreated LSEC at 0h, 48h, 30min, 6h, 24h supernatant (pg/mL) (A) and lysate (pg/mL) (B) samples. Error bar: SEM; n=3

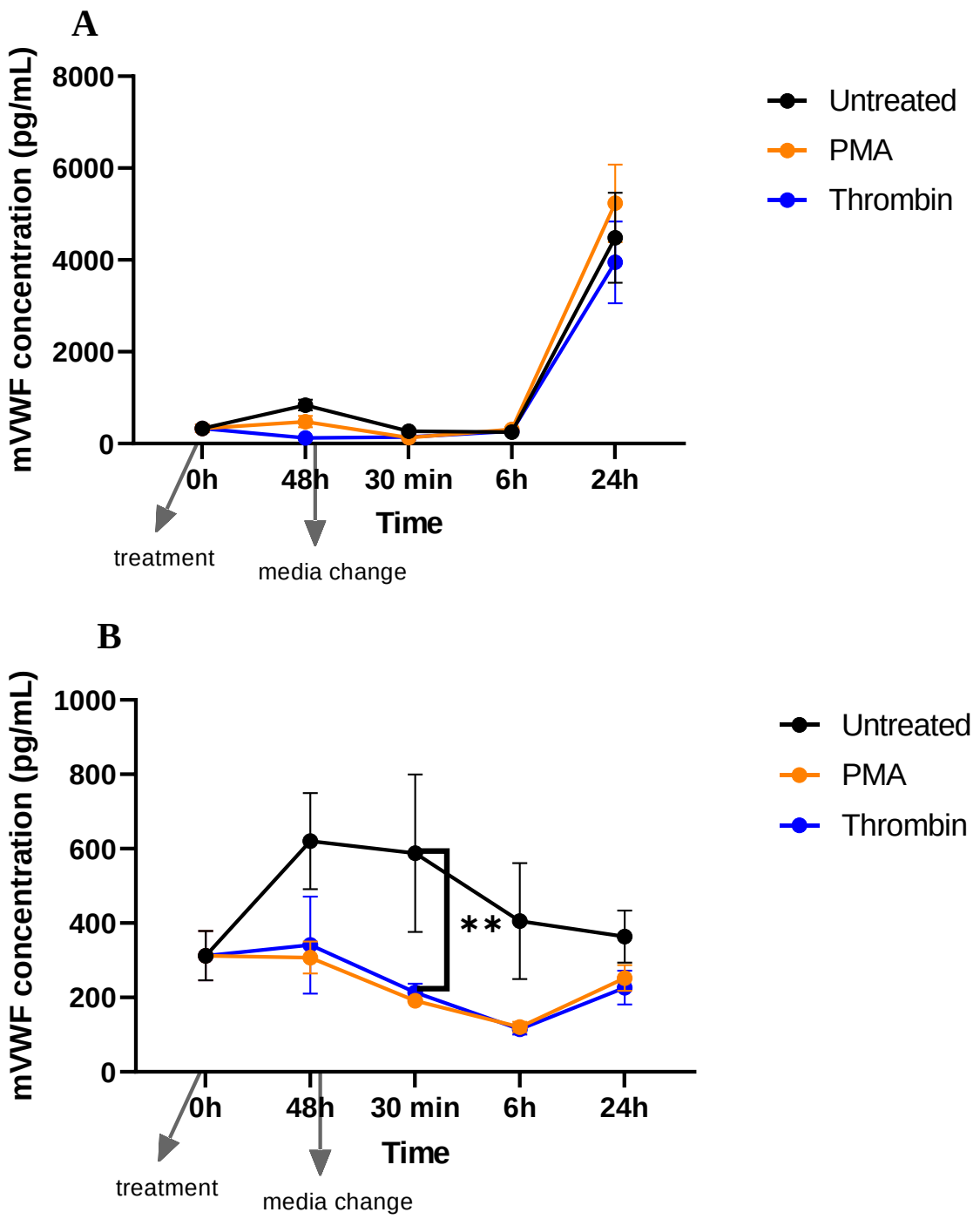

Figure 7. LSEC was grown to 30% confluency and lysate and supernatant samples were collected. At this point, cells were left untreated or treated with 100ng/mL PMA or 2IU/mL thrombin. After incubating for 48h, supernatant and lysates were collected, and media was replaced with fresh media. 30 minutes, 6h and 24h after media was changed, supernatant and lysate samples were collected, and ELISA was performed. This figure represents mVWF concentration of untreated, PMA-treated, and thrombin-treated LSEC at 0h, 48h, 30min, 6h, 24h supernatant (pg/mL) (A) and lysate (pg/mL) (B) samples. Error bar: SEM (Figure B: *P=.0087 thrombin; P=0.0041 PMA);* n= 6

3.1.2 LMEC

Figure 8a demonstrates a similar increase to the LSEC at 24 hours for the LMEC supernatant, however no decrease was demonstrated post-media change. Figure 8b demonstrates no overall increase in mVWF in lysates, however there is an increase between 48 and 6-hour timepoints.

Like the LSEC, the LMEC showed no increase in mVWF between control versus treated cells of the lysates and supernatant; however, there is an increase demonstrated for both PMA and thrombin treated cells at 24 hours in the supernatant (figure 9).

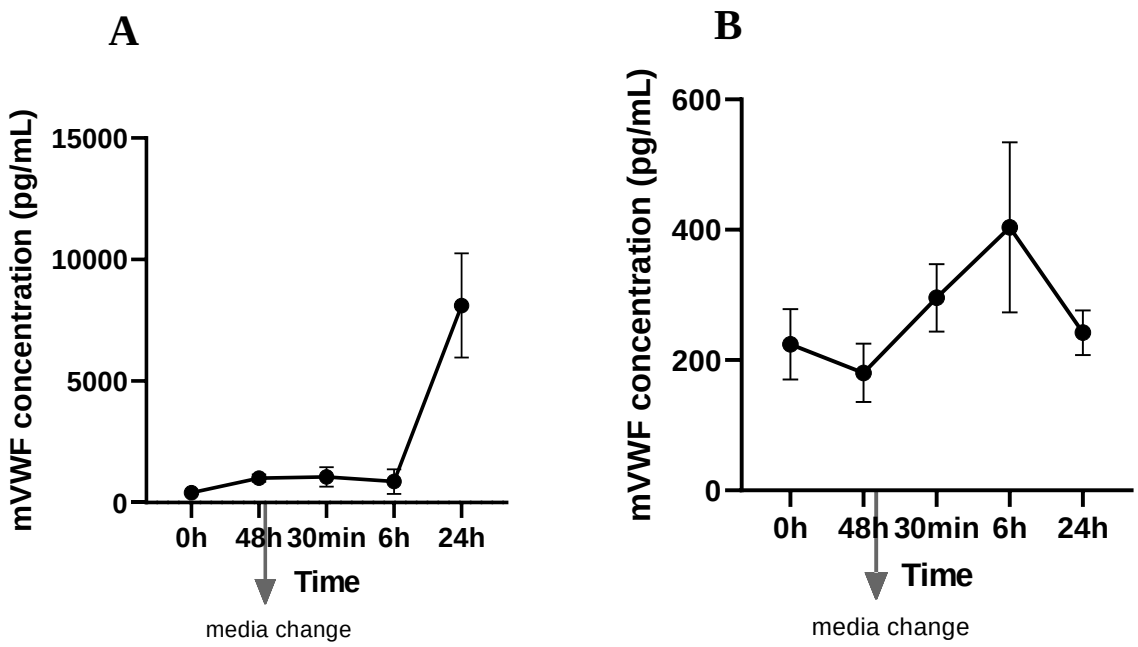

Figure 8. Untreated LMEC were grown to 30% confluency (0h) and samples were collected. Samples were then collected 48h later, and media was replaced. 30 minutes, 6h and 24h after media was changed, supernatant and lysate samples were collected, and ELISA was performed. This figure demonstrates mVWF concentration of untreated LMEC at 0h, 48h, 30min, 6h, 24h supernatant (pg/mL) (A) and lysate (pg/mL) (B) samples. Error bar: SEM; n=3

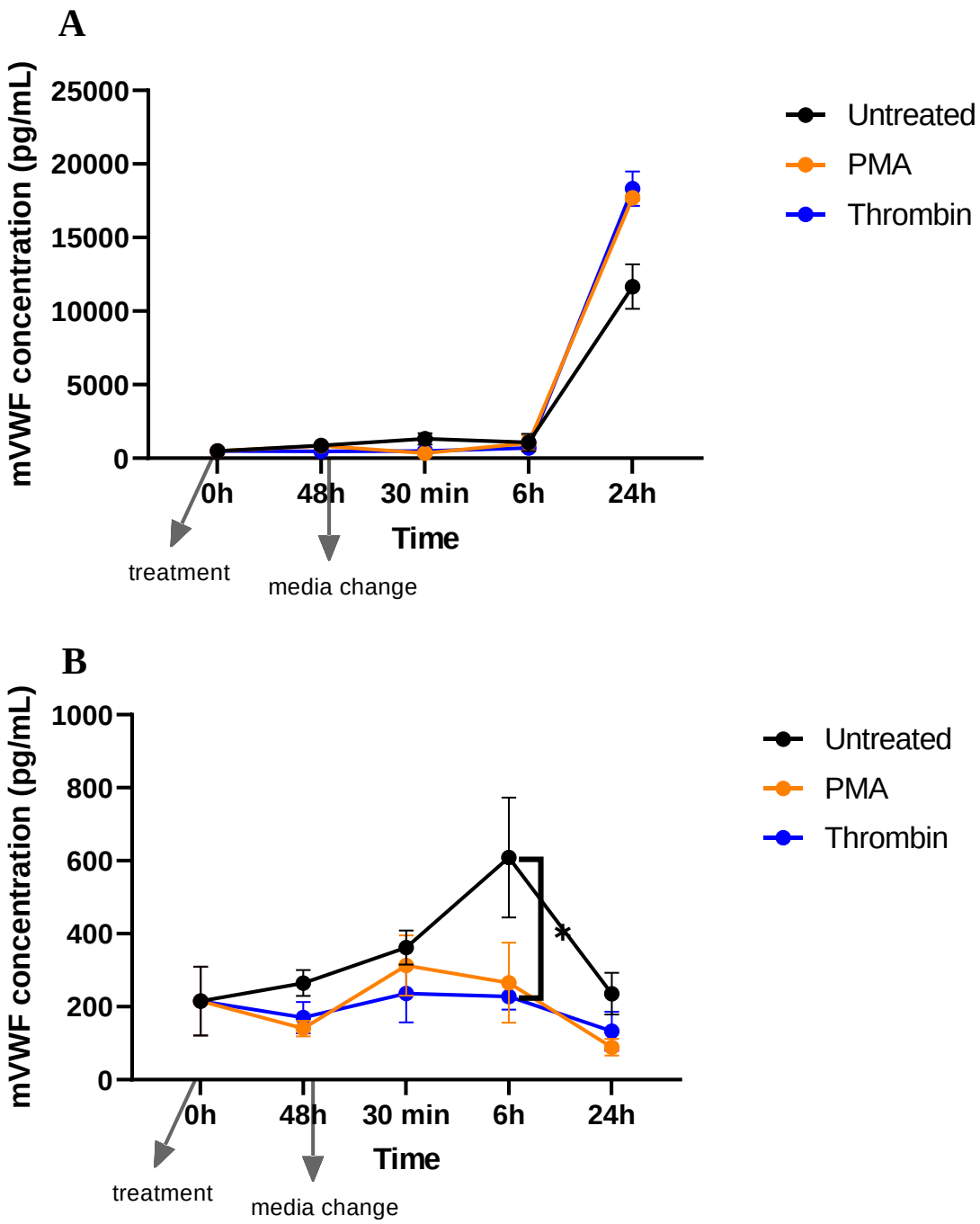

Figure 9. LMEC was grown to 30% confluency and lysate and supernatant samples were collected. At this point, cells were left untreated or treated with 100ng/mL PMA or 2IU/mL thrombin. After incubating for 48h, supernatant and lysates were collected, and media was replaced with fresh media. 30 minutes, 6h and 24h after media was changed, supernatant and lysate samples were collected, and ELISA was performed. This figure represents mVWF concentration of untreated, PMA-treated, and thrombin-treated LMEC at 0h, 48h, 30min, 6h, 24h supernatant (pg/mL) (A) and lysate (pg/mL) (B) samples. Error bar: SEM (Figure B: Thrombin: *P=.0273, PMA:.0284);* n= 6

3.1.3 iMAEC

Figure 10a demonstrates an overall increase in mVWF from 0 hours to 24 hours in iMAEC supernatant, like the LSEC supernatant. Like LSEC supernatant, there was also a decrease in mVWF at the 30 minutes after the media change. However, there is no overall increase in VWF seen in the lysates of the iMAEC (figure 10b).

Like the LSEC, the iMAEC also demonstrated no increase in mVWF when comparing untreated to treated supernatant and lysates (figure 11). Interestingly, there seems to be an increase in VWF in the untreated control versus treated lysates for all three mouse cell lines.

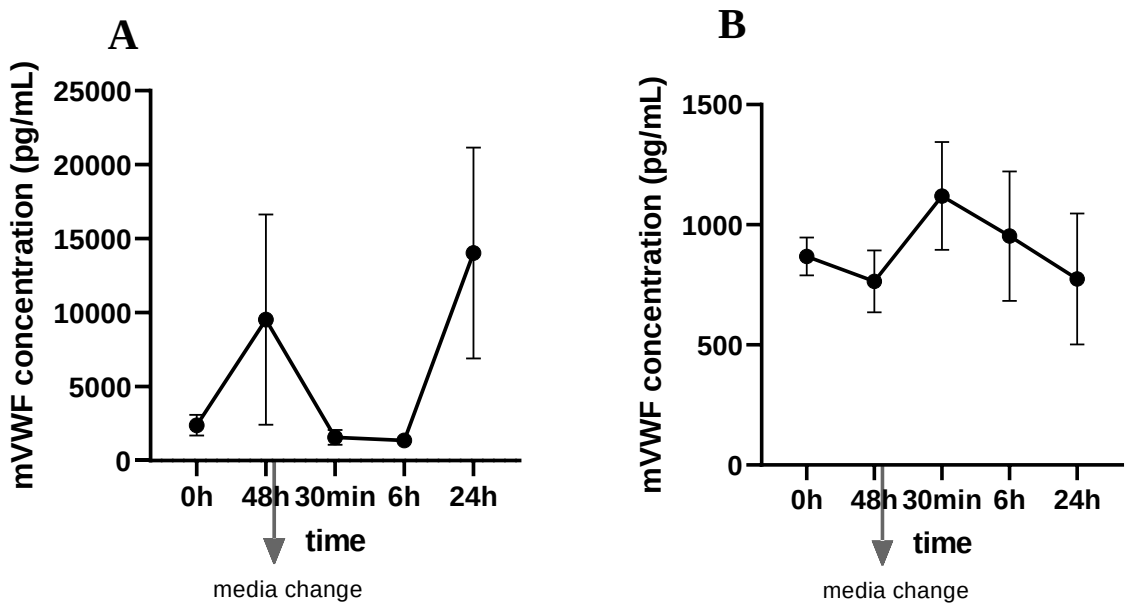

Figure 10. Untreated iMAEC were grown to 30% confluency (0h) and samples were collected. Samples were then collected 48h later, and media was replaced. 30 minutes, 6h and 24h after media was changed, supernatant and lysate samples were collected, and ELISA was performed. This figure demonstrates mVWF concentration of untreated iMAEC at 0h, 48h, 30min, 6h, 24h supernatant (pg/mL) (A) and lysate (pg/mL) (B) samples. Error bar: SEM; n=3

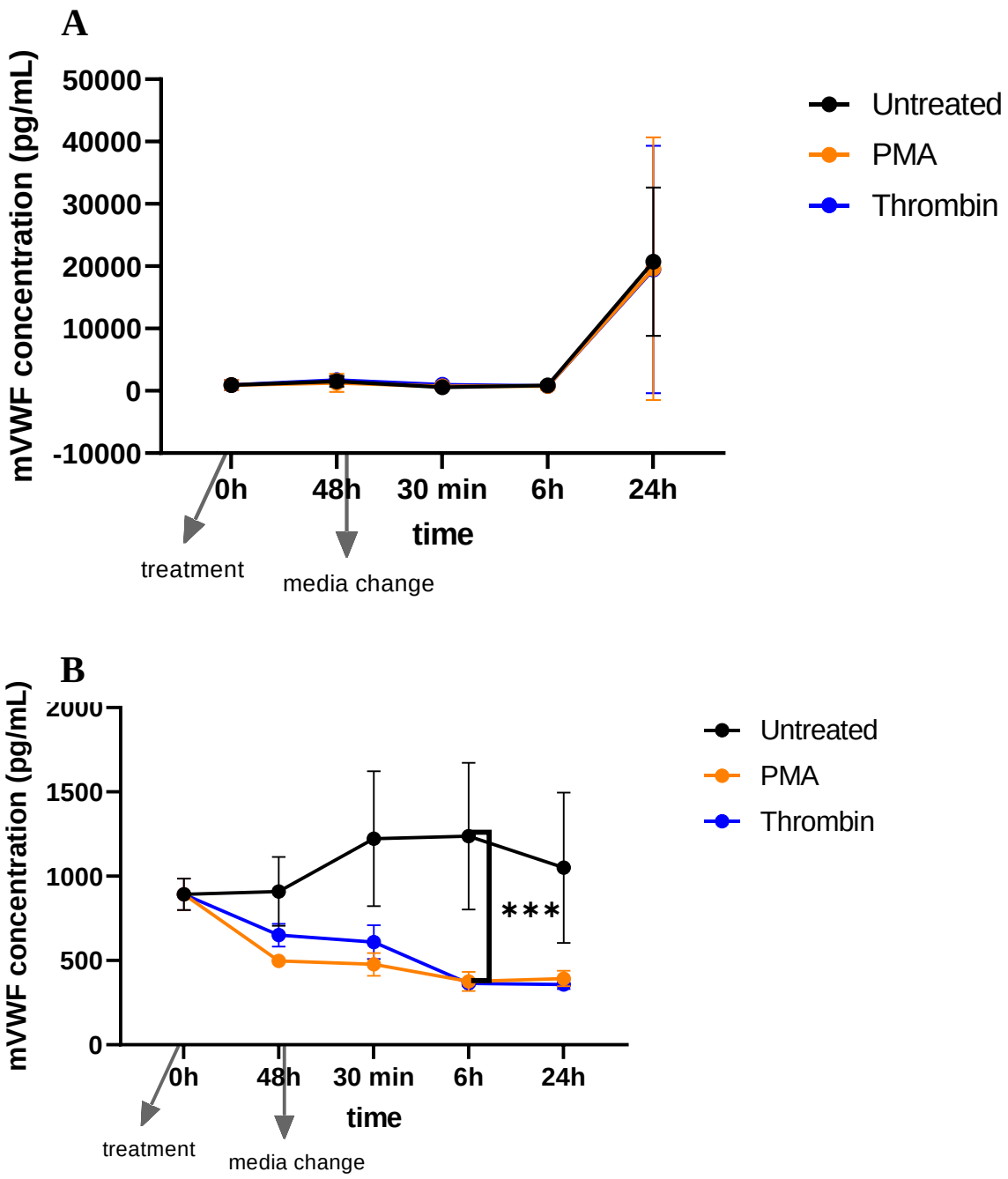

Figure 11. iMAEC was grown to 30% confluency and lysate and supernatant samples were collected. At this point, cells were left untreated or treated with 100ng/mL PMA or 2IU/mL thrombin. After incubating for 48h, supernatant and lysates were collected, and media was replaced with fresh media. 30 minutes, 6h and 24h after media was changed, supernatant and lysate samples were collected, and ELISA was performed. This figure represents mVWF concentration of untreated, PMA-treated, and thrombin-treated iMAEC at 0h, 48h, 30min, 6h, 24h supernatant (pg/mL) (A) and lysate (pg/mL) (B) samples. Error bar: SEM (Figure B: *P=.0002 thrombin; P=0.0001 PMA);* n= 6

The HUVEC supernatant, like the LSEC and the iMAEC, there is a decrease in VWF after the media change at 30 minutes (figure 12a), however, there was no overall increase in VWF from 0 hours to 24 hours. There was also no overall increase seen in the lysates of the HUVEC, with figure 12b demonstrating a slight decrease in VWF from the 48-hour time point to the 24-hour time point.

Figure 13a demonstrates a slight increase in VWF in the supernatant of HUVEC at the 48 hours timepoint, right before the media change for treated versus untreated cells. Figure 13b demonstrates and increase in VWF for thrombin-treated cells at 48 hours versus PMA-treated and untreated lysates.

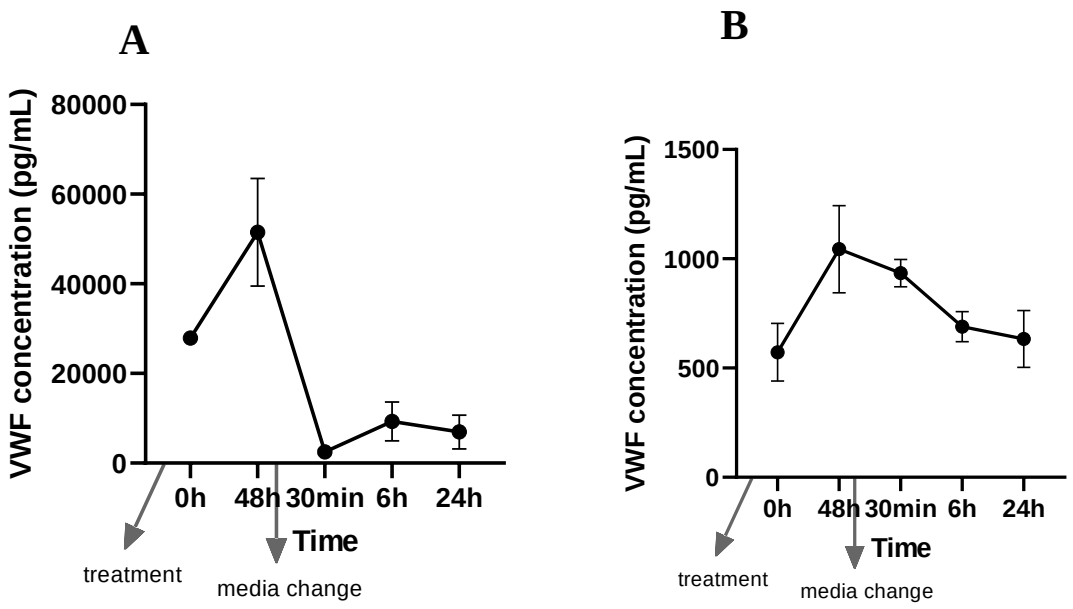

Figure 12. Untreated HUVEC were grown to 30% confluency (0h) and samples were collected. Samples were then collected 48h later, and media was replaced. 30 minutes, 6h and 24h after media was changed, supernatant and lysate samples were collected, and ELISA was performed. This figure demonstrates mVWF concentration of untreated HUVEC at 0h, 48h, 30min, 6h, 24h supernatant (pg/mL) (A) and lysate (pg/mL) (B) samples. Error bar: SEM; n=3

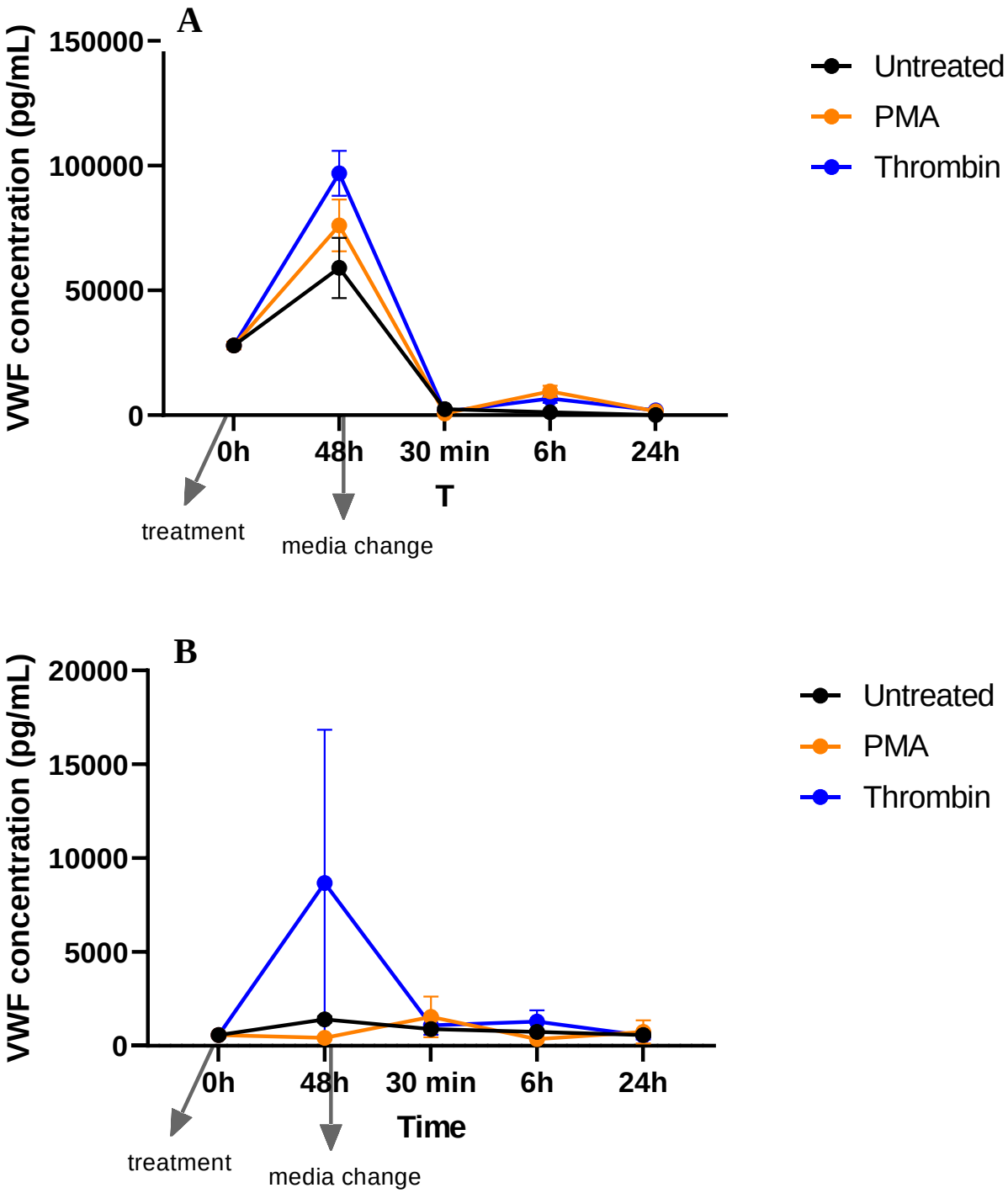

Figure 13. HUVEC was grown to 30% confluency and lysate and supernatant samples were collected. At this point, cells were left untreated or treated with 100ng/mL PMA or 2IU/mL thrombin. After incubating for 48h, supernatant and lysates were collected, and media was replaced with fresh media. 30 minutes, 6h and 24h after media was changed, supernatant and lysate samples were collected, and ELISA was performed. This figure represents mVWF concentration of untreated, PMA-treated, and thrombin-treated HUVEC at 0h, 48h, 30min, 6h, 24h supernatant (pg/mL) (A) and lysate (pg/mL) (B) samples. Error bar: SEM; n= 6

3.2 Fold-change of VWF RNA expression

After culturing LSEC, LMEC, iMAEC and HUVEC, the were left untreated, treated with PMA, and treated with thrombin at 30% confluency. 48 hours after cells were treated, cells were washed, and media was replaced with fresh media. 48-hour time point RNA lysate sample was collected immediately before changing media. After changing media, the same samples were collected at 30-minute, 6-hour, and 24-hour timepoints. RNA was extracted from these samples and a reverse transcription reaction was performed for cDNA synthesis. The resulting cDNA was quantified using qPCR and fold-change between the treated and untreated samples was calculated. A comparison of relative expression of control samples in all cell lines and fold change in all cell lines is demonstrated in Table S2a-b.

3.2.1 LSEC

Figure 14 demonstrates that there is an upregulation of VWF expression when treated with PMA at 48h post-treatment and 30 minutes post-media change. However, there does not seem to be an upregulation or downregulation of expression at the 6h and 24h timepoints or for any of the thrombin-treated samples.

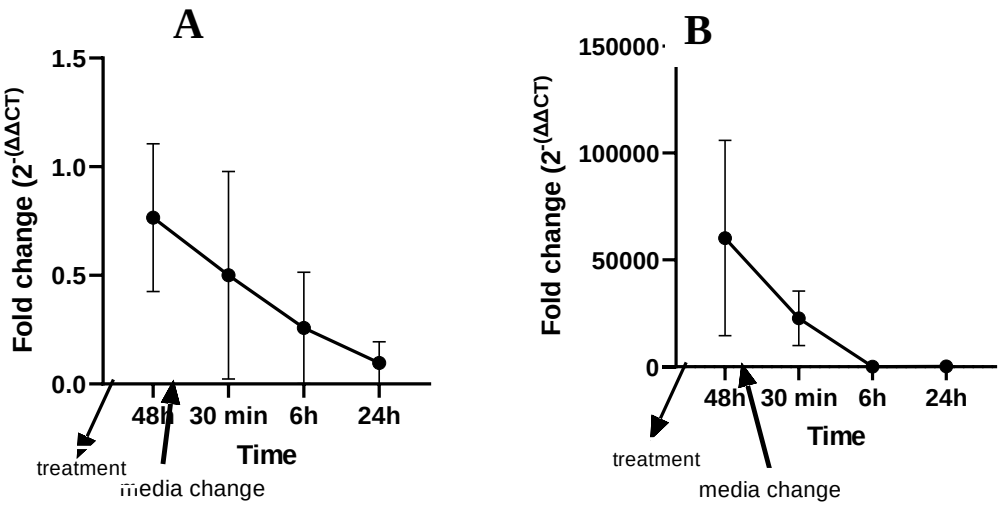

Figure 14. LSEC was grown to 30% and were left untreated or treated with 100ng/mL PMA or 2IU/mL thrombin. After incubating for 48h, cells were collected, and media was replaced with fresh media. 30 minutes, 6h and 24h after media was changed, cells were collected. RNA was isolated from collected cells and reverse transcription to cDNA was performed. cDNA was used to perform qPCR with housekeeping (B-Actin) and test (VWF) primers to obtain Ct values. Ct values were used to calculate fold change between untreated and treated samples. This figure represents VWF fold change of A) PMA-treated and B) thrombin-treated LSEC compared to untreated LSEC at 0h, 48h, 30min, 6h, 24h samples. Error bar: SEM; n=3

3.2.2 LMEC

Figure 15 demonstrates an overall upregulation of VWF expression for PMA and thrombin-treated samples in the LMEC. There appears to be a general decrease in the expression over time for the PMA-treated samples whereas the thrombin-treated samples seem to have a slight increase over time.

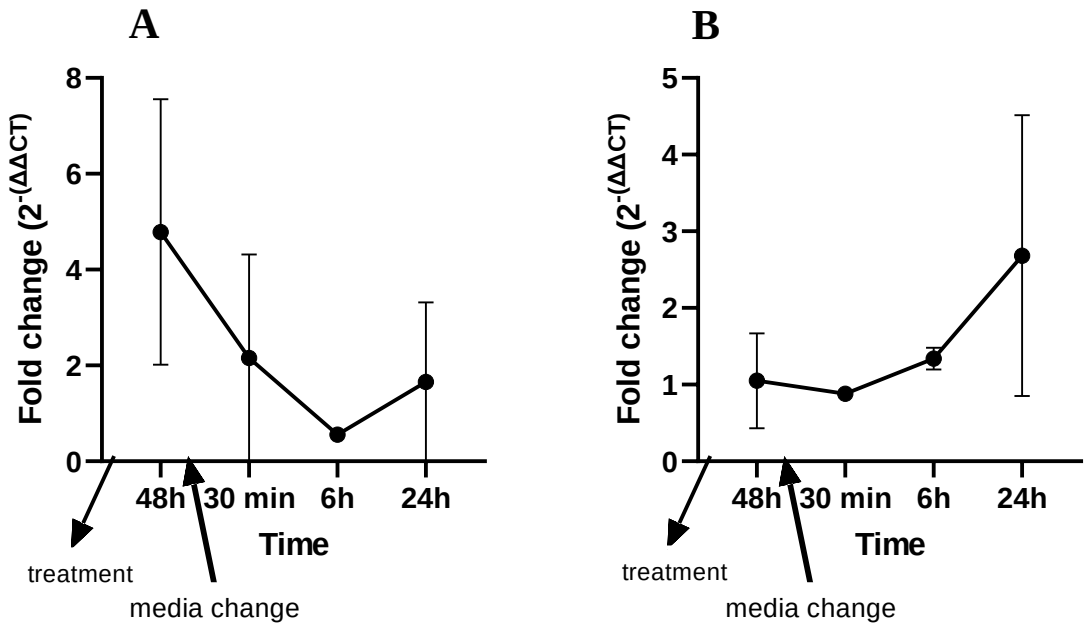

Figure 15. LMEC was grown to 30% and were left untreated or treated with 100ng/mL PMA or 2IU/mL thrombin. After incubating for 48h, cells were collected, and media was replaced with fresh media. 30 minutes, 6h and 24h after media was changed, cells were collected. RNA was isolated from collected cells and reverse transcription to cDNA was performed. cDNA was used to perform qPCR with housekeeping (B-Actin) and test (VWF) primers to obtain Ct values. Ct values were used to calculate fold change between untreated and treated samples. This figure represents VWF fold change of A) PMA-treated and B) thrombin-treated LMEC compared to untreated LSEC at 0h, 48h, 30min, 6h, 24h samples. Error bar: SEM; n=3

3.2.3 iMAEC

Like the LMEC, the iMAEC also demonstrate an overall upregulation of VWF expression for both of the treated groups (figure 16) Like the LMEC, there was an overall decrease in the expression over time for PMA-treated samples, however, in this case there was also a decrease over time for thrombin-treated samples.

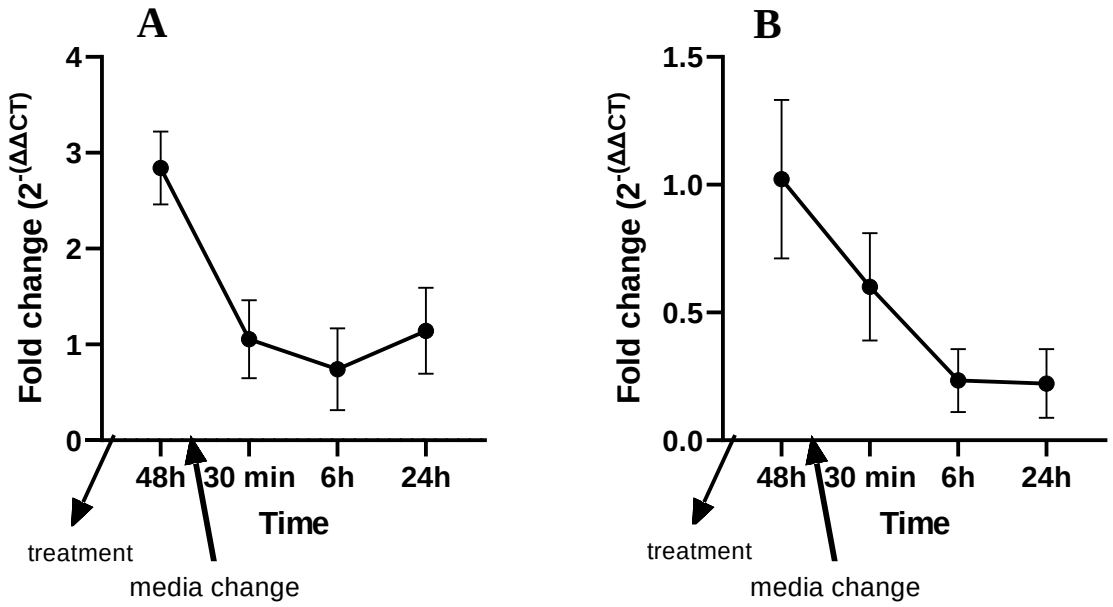

Figure 16. iMAEC was grown to 30% and were left untreated or treated with 100ng/mL PMA or 2IU/mL thrombin. After incubating for 48h, cells were collected, and media was replaced with fresh media. 30 minutes, 6h and 24h after media was changed, cells were collected. RNA was isolated from collected cells and reverse transcription to cDNA was performed. cDNA was used to perform qPCR with housekeeping (B-Actin) and test (VWF) primers to obtain Ct values. Ct values were used to calculate fold change between untreated and treated samples. This figure represents VWF fold change of A) PMA-treated and B) thrombin-treated iMAEC compared to untreated LSEC at 0h, 48h, 30min, 6h, 24h samples. Error bar: SEM; n=3

3.2.4 HUVEC

Figure 17 demonstrates that the HUVECs show a similar expression pattern to the LSEC. Like the LSEC, there is an upregulation in VWF expression at 48h and no upregulation at the 6h and 24h timepoints for PMA-treated samples. There is also no upregulation or downregulation for thrombin-treated samples. Unlike the LSEC, there is no upregulation at the 30-minute timepoint for PMA-treated HUVECs.

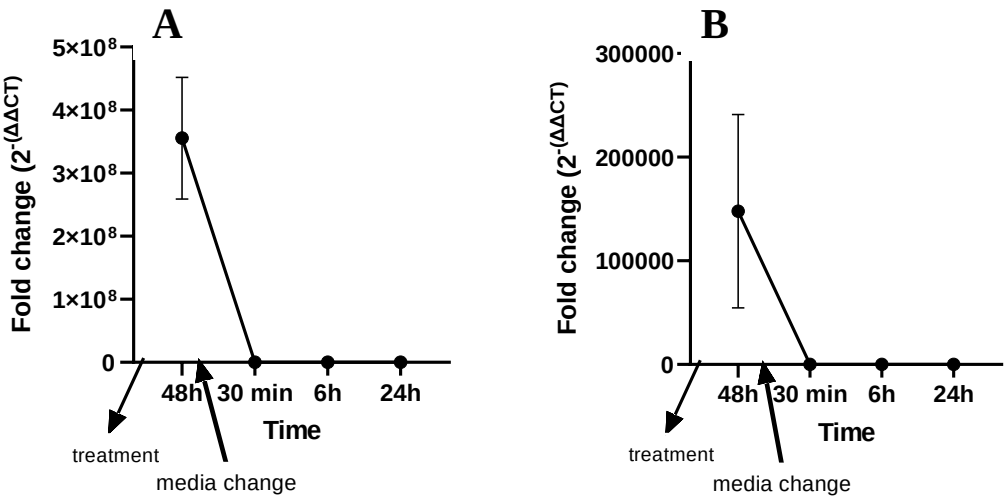

Figure 17. HUVEC was grown to 30% and were left untreated or treated with 100ng/mL PMA or 2IU/mL thrombin. After incubating for 48h, cells were collected, and media was replaced with fresh media. 30 minutes, 6h and 24h after media was changed, cells were collected. RNA was isolated from collected cells and reverse transcription to cDNA was performed. cDNA was used to perform qPCR with housekeeping (B-Actin) and test (VWF) primers to obtain Ct values. Ct values were used to calculate fold change between untreated and treated samples. This figure represents VWF fold change of A) PMA-treated and B) thrombin-treated HUVEC compared to untreated LSEC at 0h, 48h, 30min, 6h, 24h samples. Error bar: SEM; n=3

3.3 Qualitative VWF expression

LSEC, LMEC, iMAEC and HUVEC, were treated with PMA and thrombin at 30% confluency. 24 hours after treatment, cells were fixed and stained for VWF, P-selectin, and DAPI.

3.3.1 LSEC

Figure 18 demonstrates clear DAPI and p-selectin staining, however VWF is not as visible for untreated LSEC. Like the untreated cells, DAPI and p-selectin was visualized for PMA and thrombin-treated LSEC, however, VWF was also better visualized at both objectives (figure 19, 20).

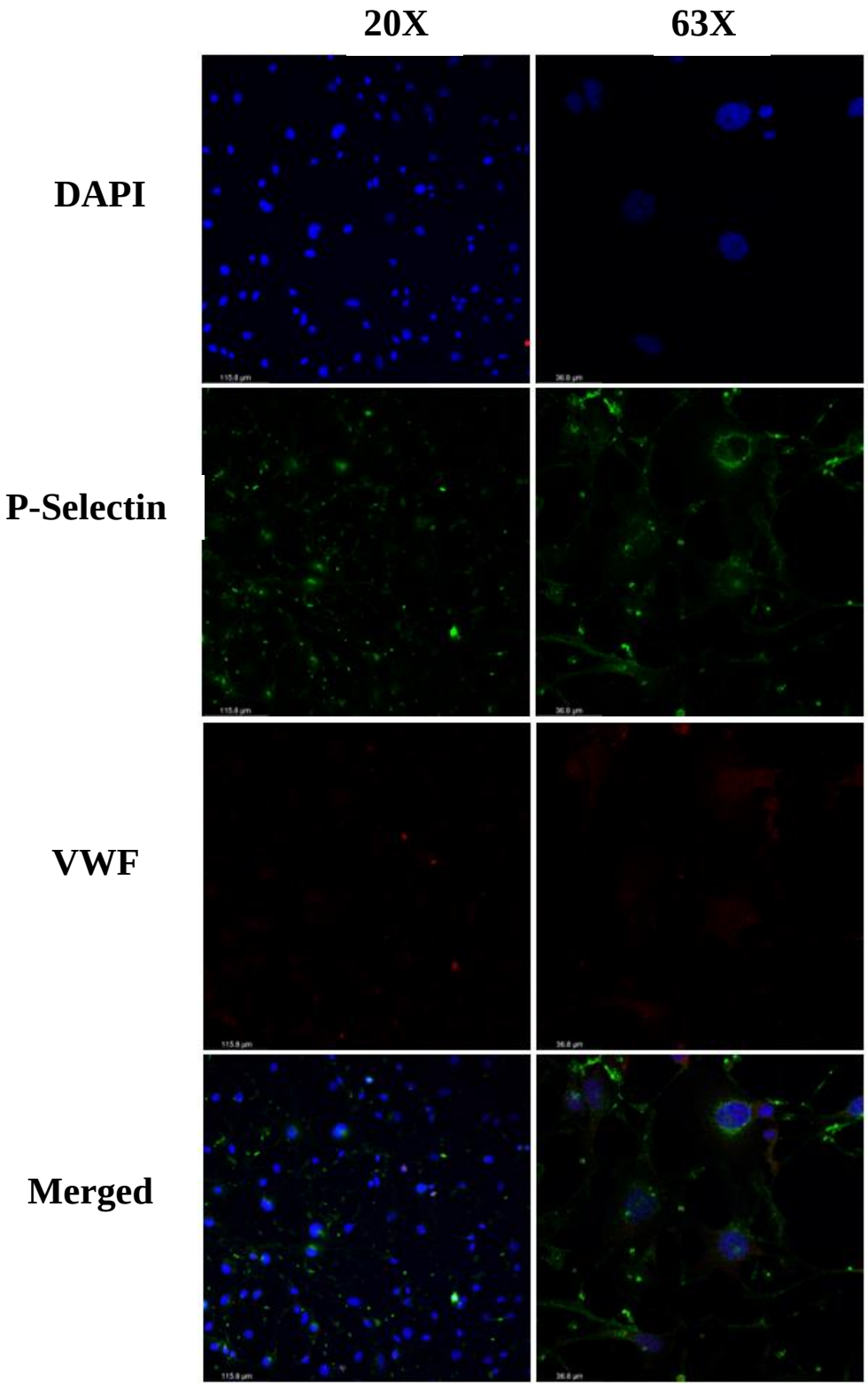

Figure 18. LSEC was grown to 50% on glass coverslips. After incubating for 24h, cells were fixed in 4% PFA, and media was replaced with fresh media. After cells were blocked, staining was performed for VWF, P-selectin and DAPI and mounted. Slides were visualized using confocal microscopy. This figure represents untreated LSEC stained with VWF, p-selectin and DAPI at 20X and 63X objectives, 24 hours after treatment.

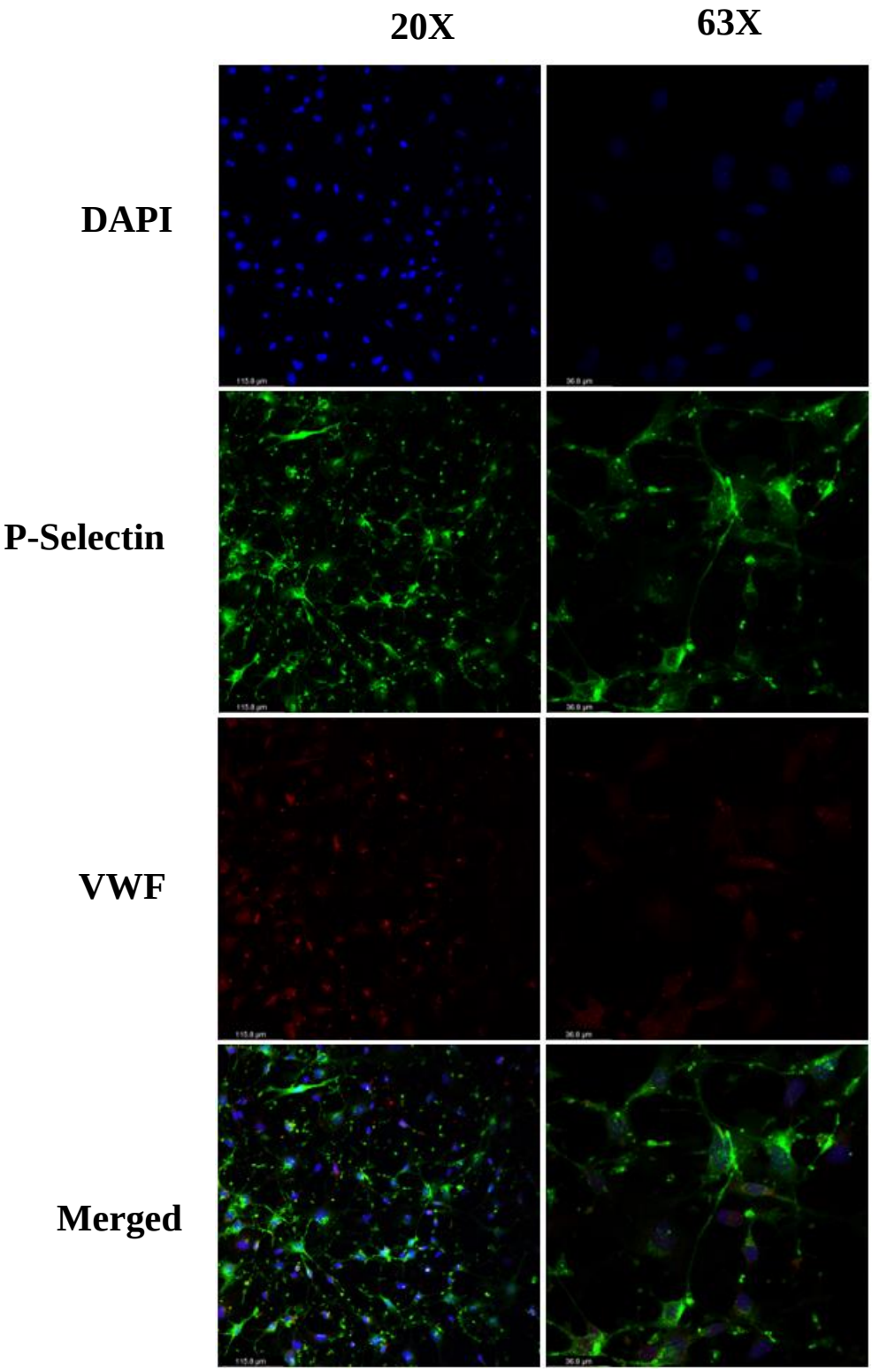

Figure 19. LSEC was grown to 50% on glass coverslips and treated with 100ng/mL PMA. After incubating for 24h, cells were fixed in 4% PFA, and media was replaced with fresh media. After cells were blocked, staining was performed for VWF, P-selectin and DAPI and mounted. Slides were visualized using confocal microscopy. This figure represents PMA-treated LSEC stained with VWF, p-selectin and DAPI at 20X and 63X objectives, 24 hours after treatment.

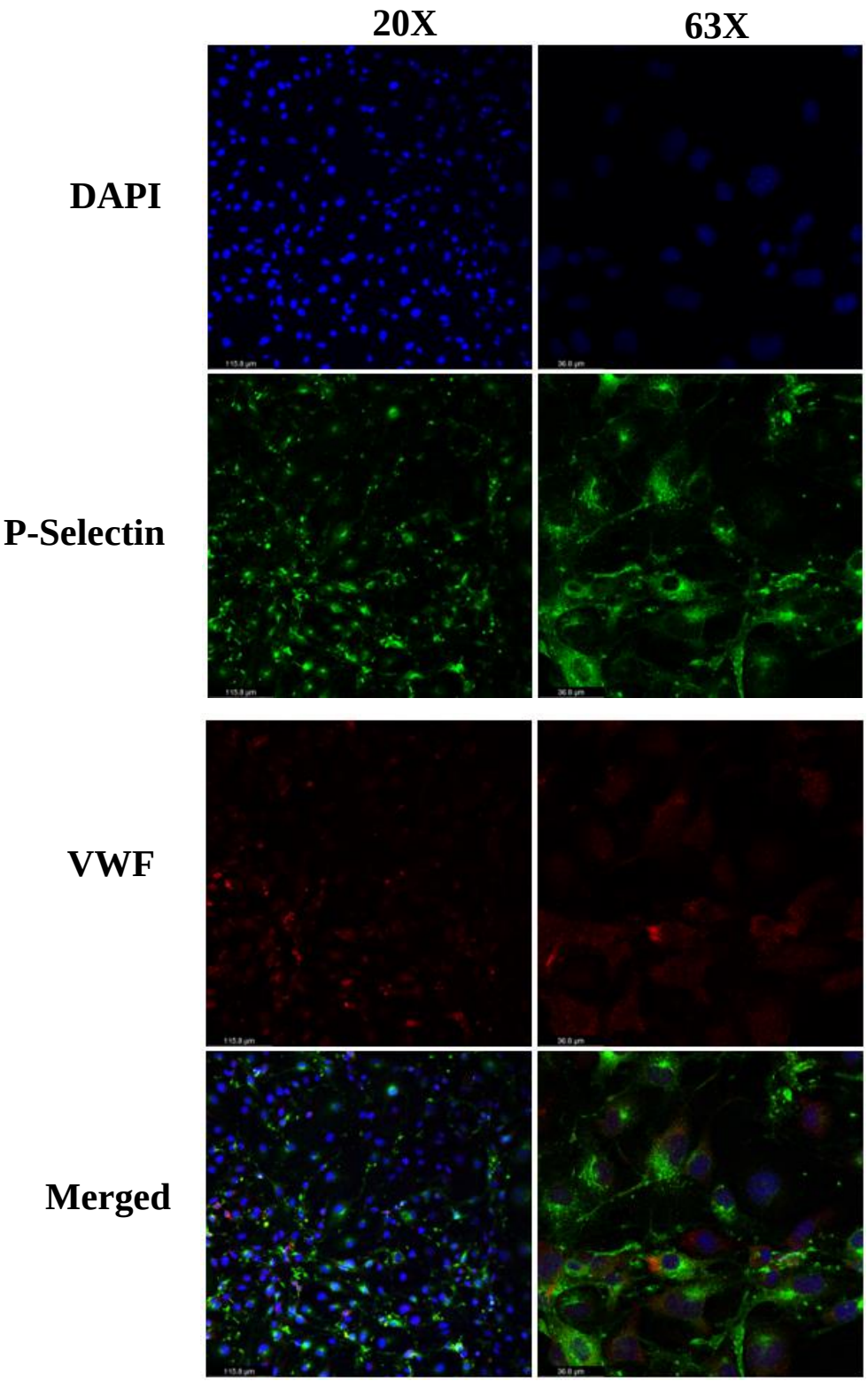

Figure 20. LSEC was grown to 50% on glass coverslips and treated with 2IU/mL thrombin. After incubating for 24h, cells were fixed in 4% PFA, and media was replaced with fresh media. After cells were blocked, staining was performed for VWF, P-selectin and DAPI and mounted. Slides were visualized using confocal microscopy. This figure represents thrombin-treated LSEC stained with VWF, p-selectin and DAPI at 20X and 63X objectives, 24 hours after treatment.

3.3.2 LMEC

Figure 21 demonstrates that like the untreated LSEC, the untreated LMEC also had clear DAPI and p-selectin staining and little VWF staining. PMA-treated LMEC was more visible by the 63X objective versus 20X objective (figure 22). For the 63X objective there is clear staining for DAPI, p-selectin and VWF. While thrombin-treated LMEC did demonstrate DAPI and P-selectin staining, there was not as much VWF staining seen (figure 23).

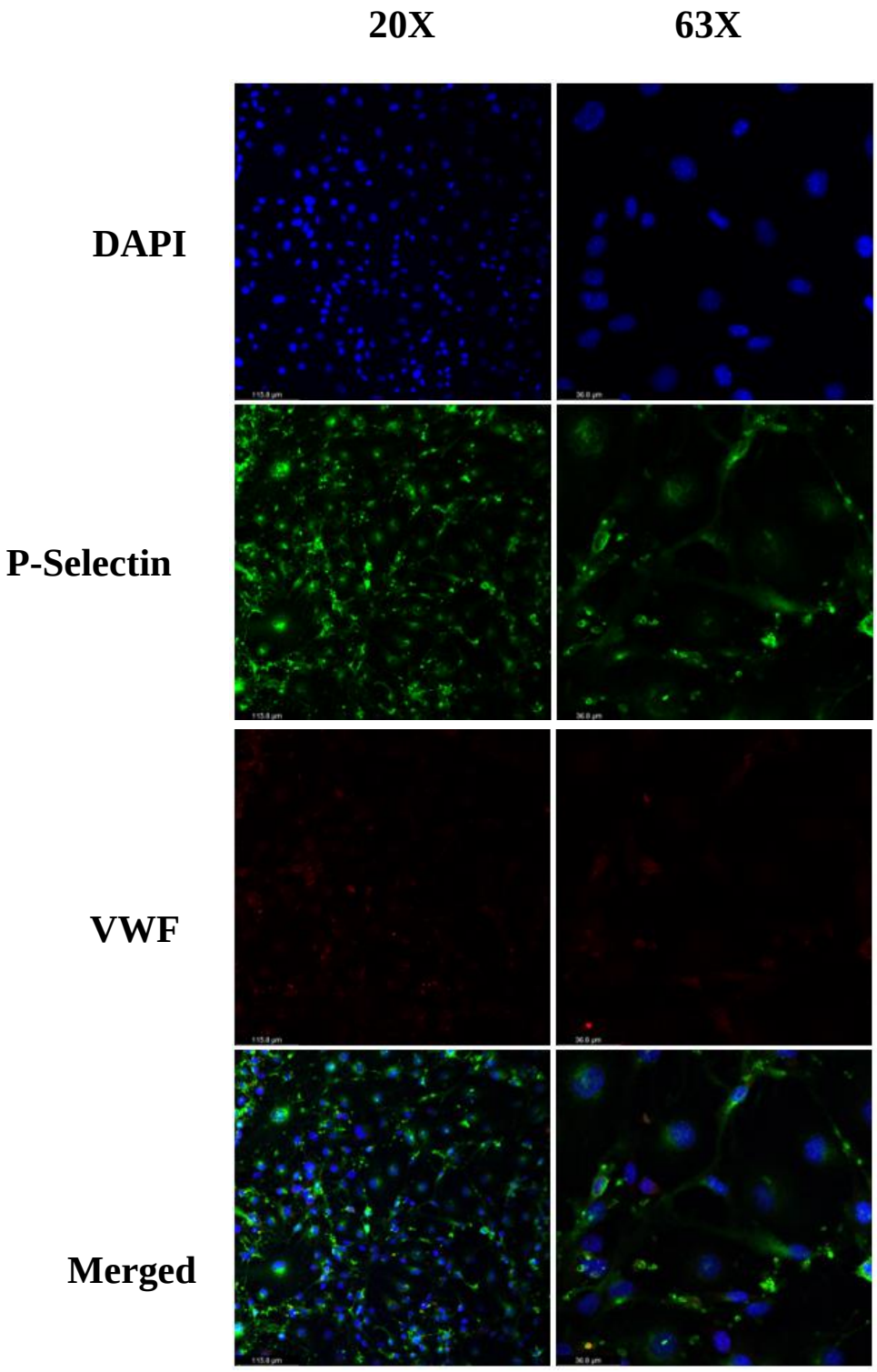

Figure 21. LMEC was grown to 50% on glass coverslips. After incubating for 24h, cells were fixed in 4% PFA, and media was replaced with fresh media. After cells were blocked, staining was performed for VWF, P-selectin and DAPI and mounted. Slides were visualized using confocal microscopy. This figure represents untreated LMEC stained with VWF, p-selectin and DAPI at 20X and 63X objectives, 24 hours after treatment.

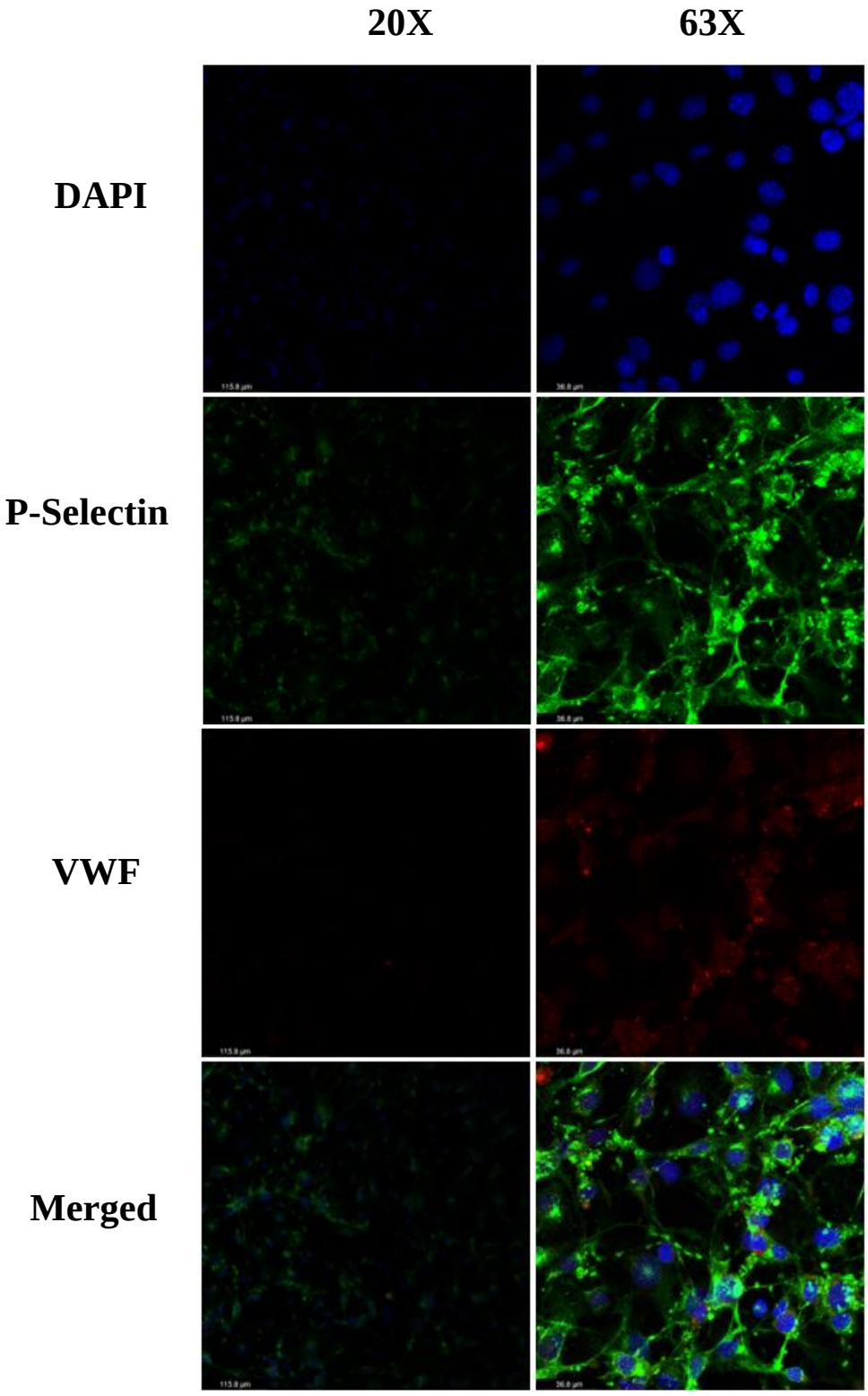

Figure 22. LMEC was grown to 50% on glass coverslips and treated with 100ng/mL PMA. After incubating for 24h, cells were fixed in 4% PFA, and media was replaced with fresh media. After cells were blocked, staining was performed for VWF, P-selectin and DAPI and mounted. Slides were visualized using confocal microscopy. This figure represents PMA-treated LMEC stained with VWF, p-selectin and DAPI at 20X and 63X objectives, 24 hours after treatment.

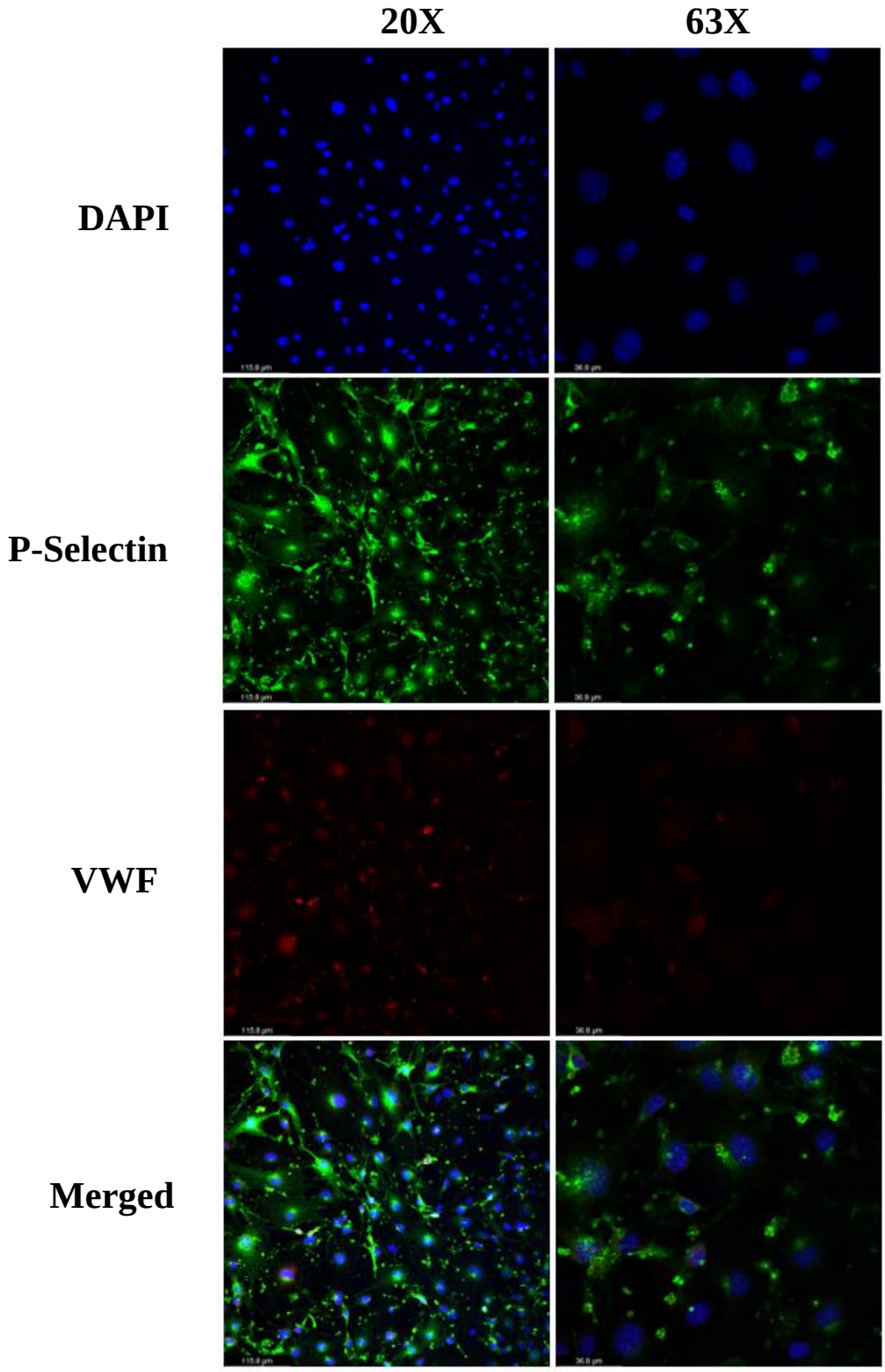

Figure 23. LMEC was grown to 50% on glass coverslips and treated with 2IU/mL thrombin. After incubating for 24h, cells were fixed in 4% PFA, and media was replaced with fresh media. After cells were blocked, staining was performed for VWF, P-selectin and DAPI and mounted. Slides were visualized using confocal microscopy. This figure represents thrombin-treated LMEC stained with VWF, p-selectin and DAPI at 20X and 63X objectives, 24 hours after treatment.

3.3.3 iMAEC

Figure 24 demonstrates staining for DAPI, p-selectin and VWF, with some potential colocalization seen for p-selectin and VWF of untreated iMAEC. Figure 25 and 26 demonstrates DAPI, p-selectin and VWF staining for PMA- and thrombin-treated iMAEC, like untreated cells.

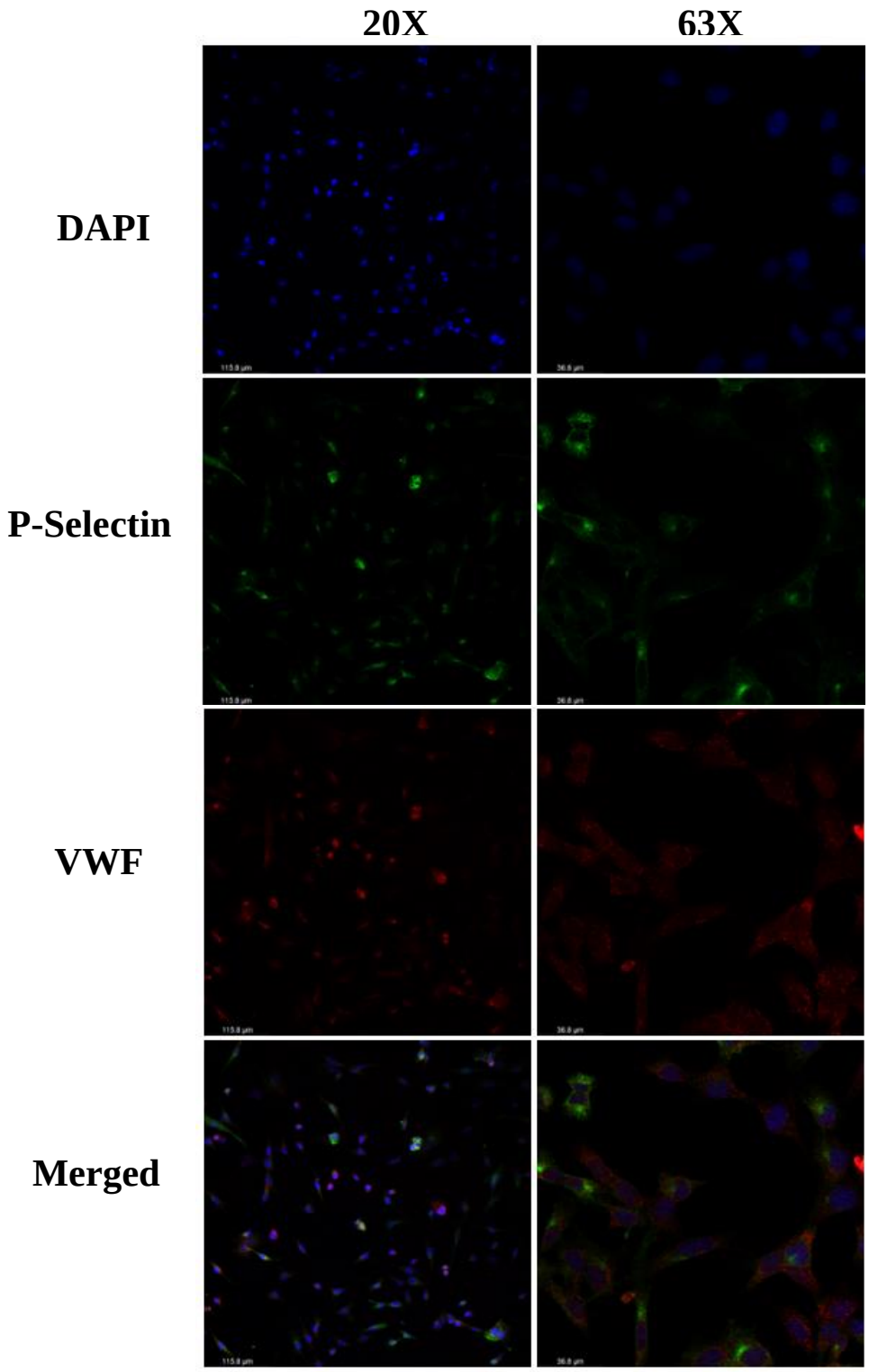

Figure 24. iMAEC was grown to 50% on glass coverslips. After incubating for 24h, cells were fixed in 4% PFA, and media was replaced with fresh media. After cells were blocked, staining was performed for VWF, P-selectin and DAPI and mounted. Slides were visualized using confocal microscopy. This figure represents untreated iMAEC stained with VWF, p-selectin and DAPI at 20X and 63X objectives, 24 hours after treatment.

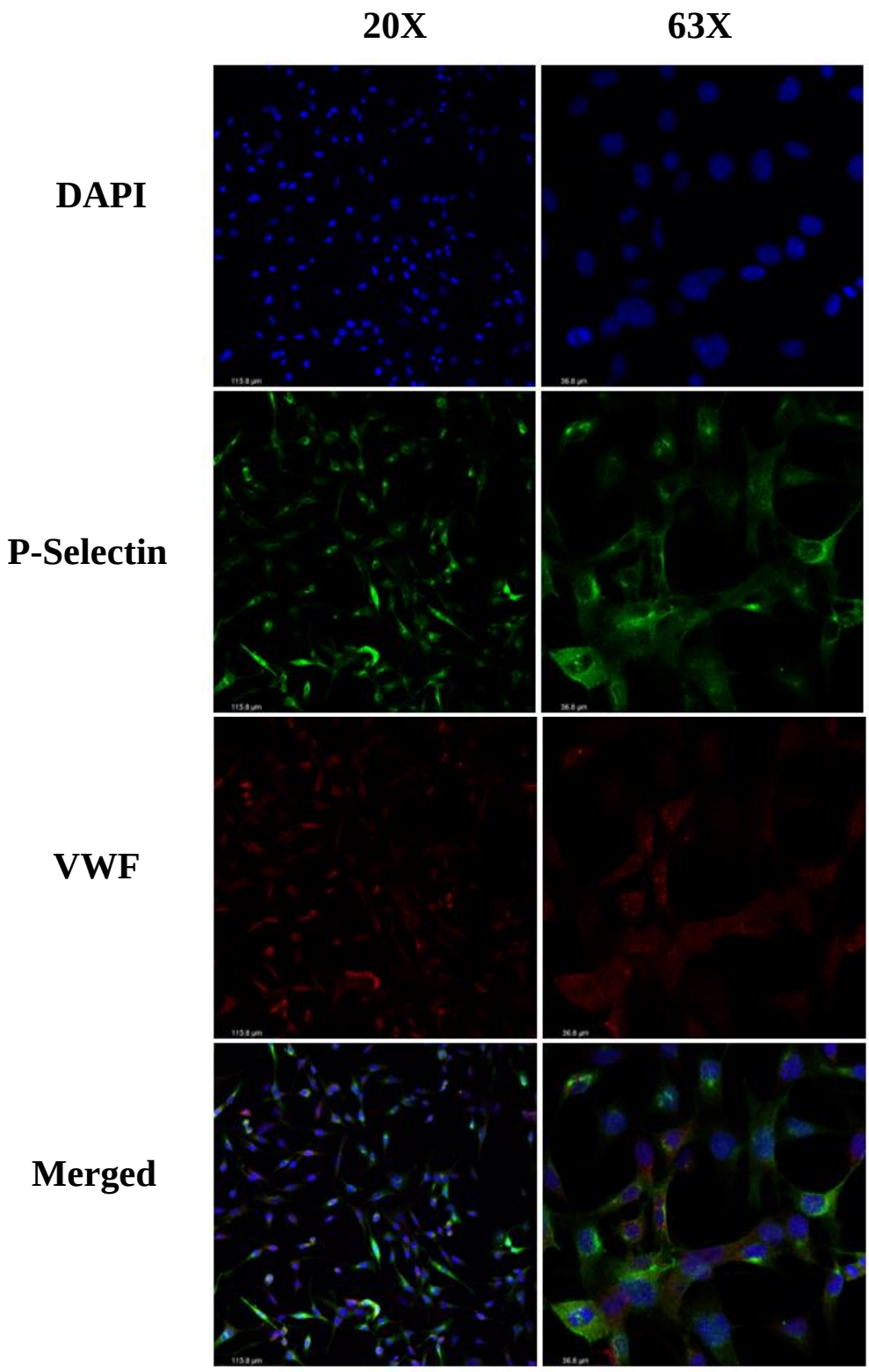

Figure 25. iMAEC was grown to 50% on glass coverslips and treated with 100ng/mL PMA. After incubating for 24h, cells were fixed in 4% PFA, and media was replaced with fresh media. After cells were blocked, staining was performed for VWF, P-selectin and DAPI and mounted. Slides were visualized using confocal microscopy. This figure represents PMA-treated iMAEC stained with VWF, p-selectin and DAPI at 20X and 63X objectives, 24 hours after treatment.

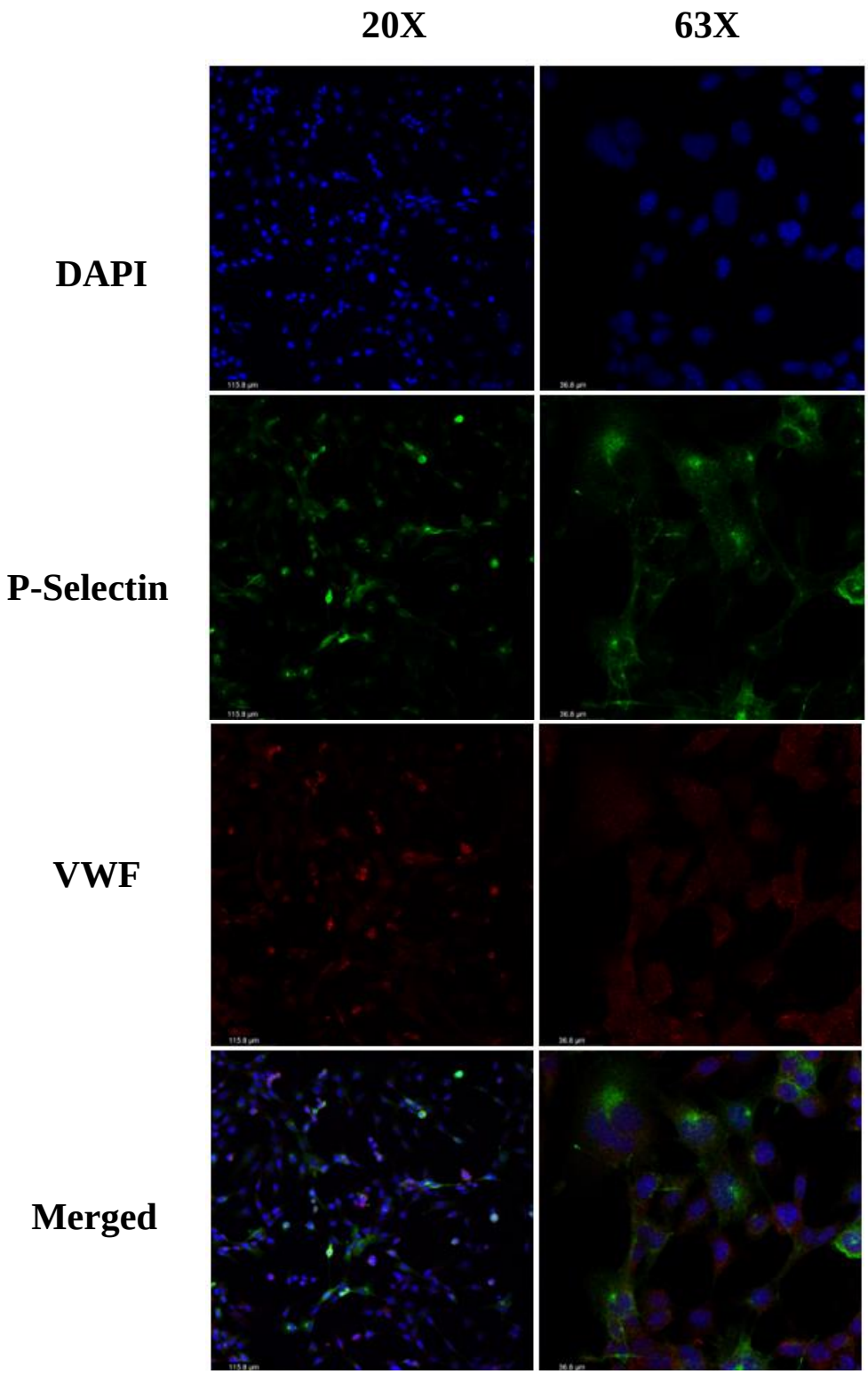

Figure 26. iMAEC was grown to 50% on glass coverslips and treated with 2IU/mL thrombin. After incubating for 24h, cells were fixed in 4% PFA, and media was replaced with fresh media. After cells were blocked, staining was performed for VWF, P-selectin and DAPI and mounted. Slides were visualized using confocal microscopy. This figure represents thrombin-treated iMAEC stained with VWF, p-selectin and DAPI at 20X and 63X objectives, 24 hours after treatment.

3.3.4 HUVEC

Figures 27-29 demonstrate some DAPI and P-selectin staining for untreated, PMA-treated, and thrombin-treated HUVEC respectively; There is also VWF staining apparent for all groups. Interestingly, you can see a clear representation of Weibel-Palade body exocytosis as indicated by the dispersing tubule-like structures (red arrows) in figure 29.

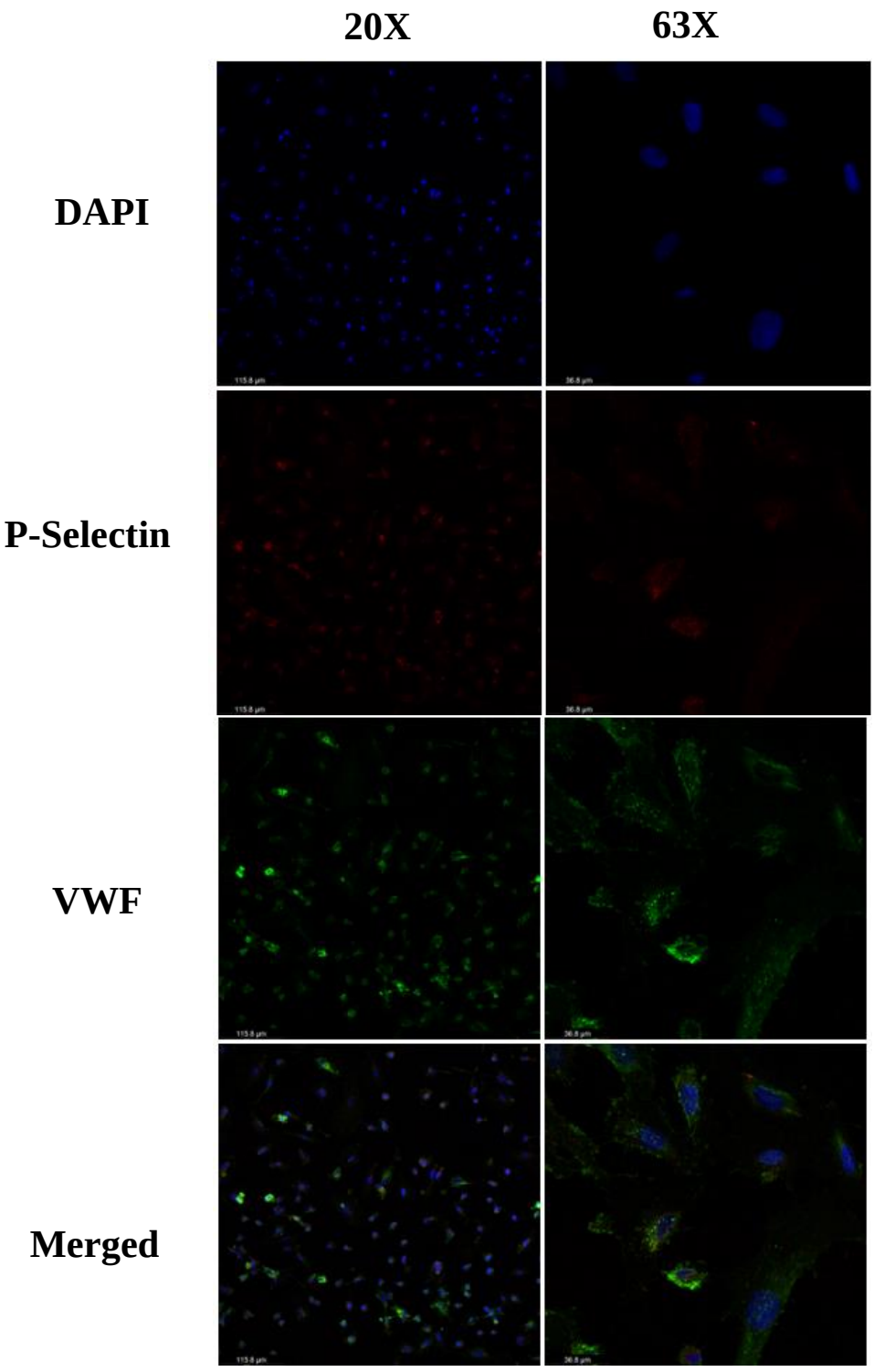

Figure 27. HUVEC was grown to 50% on glass coverslips. After incubating for 24h, cells were fixed in 4% PFA, and media was replaced with fresh media. After cells were blocked, staining was performed for VWF, P-selectin and DAPI and mounted. Slides were visualized using confocal microscopy. This figure represents untreated HUVEC stained with VWF, p-selectin and DAPI at 20X and 63X objectives, 24 hours after treatment.

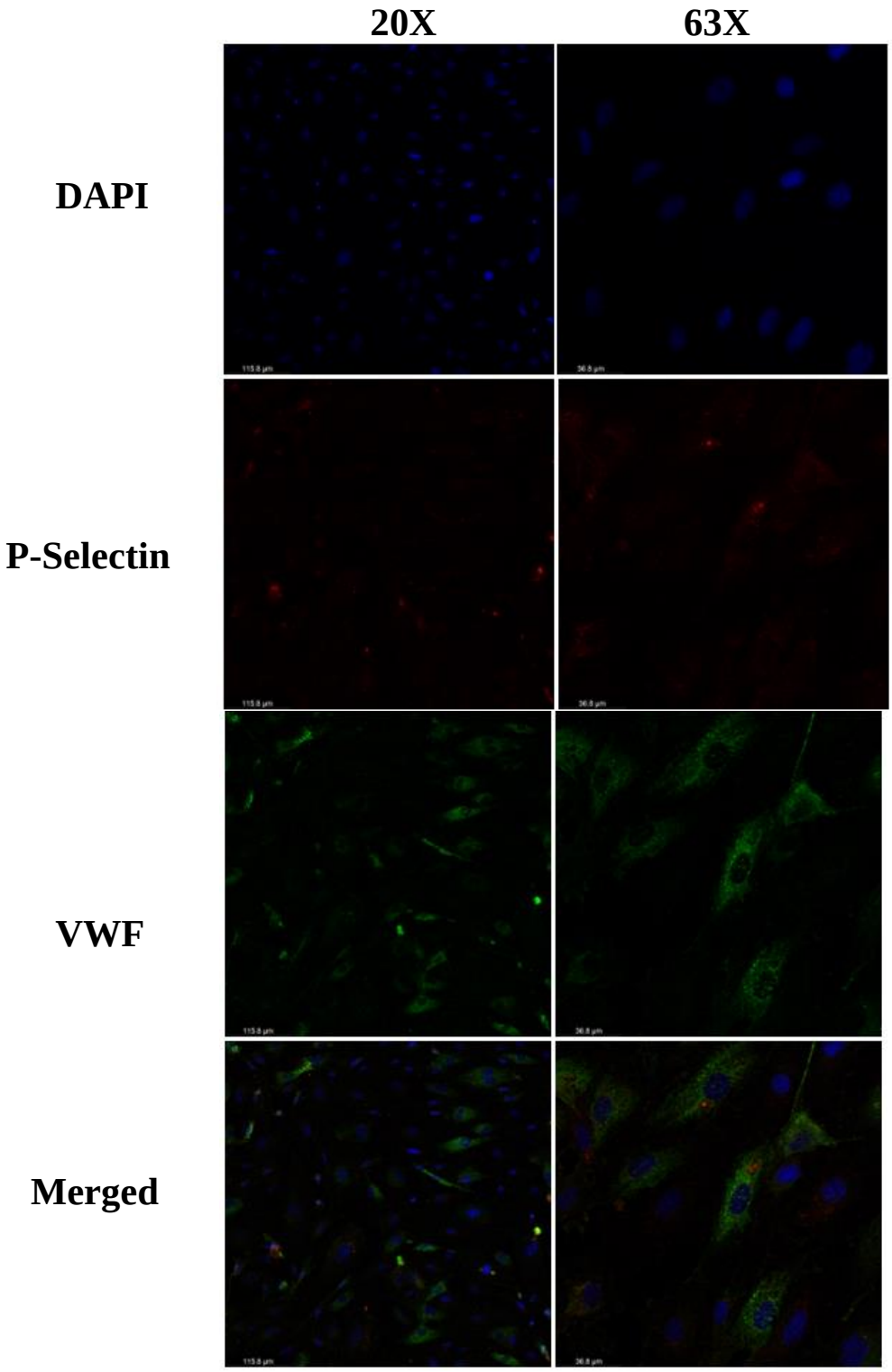

Figure 28. HUVEC was grown to 50% on glass coverslips and treated with 100ng/mL PMA. After incubating for 24h, cells were fixed in 4% PFA, and media was replaced with fresh media. After cells were blocked, staining was performed for VWF, P-selectin and DAPI and mounted. Slides were visualized using confocal microscopy. This figure represents PMA-treated HUVEC stained with VWF, p-selectin and DAPI at 20X and 63X objectives, 24 hours after treatment.

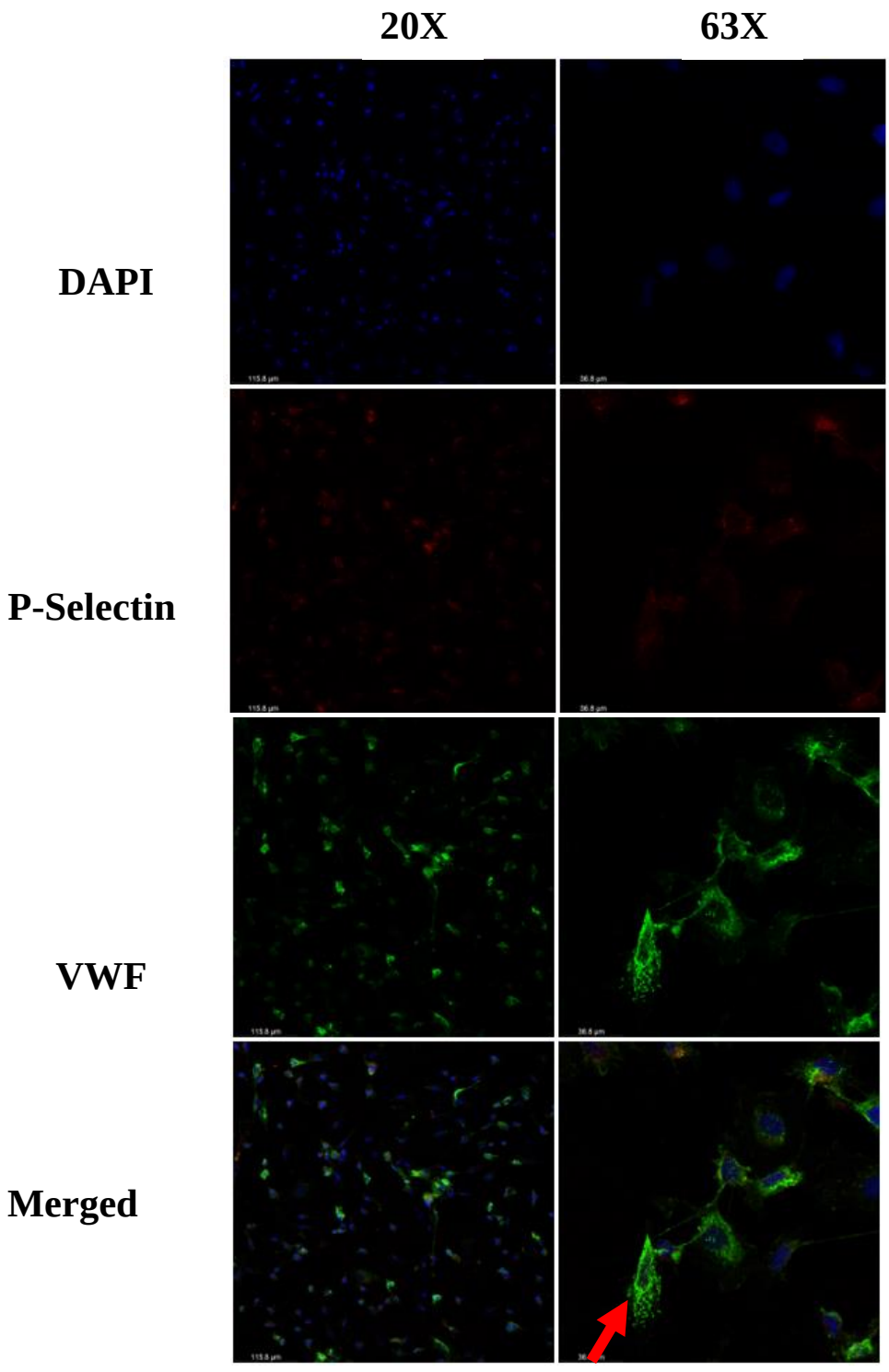

Figure 29. HUVEC was grown to 50% on glass coverslips and treated with 2IU/mL thrombin. After incubating for 24h, cells were fixed in 4% PFA, and media was replaced with fresh media. After cells were blocked, staining was performed for VWF, P-selectin and DAPI and mounted. Slides were visualized using confocal microscopy. This figure represents thrombin-treated HUVEC stained with VWF, p-selectin and DAPI at 20X and 63X objectives, 24 hours after treatment. WPBs are indicated with a red arrow.

3.4 HEK293T expressing mVWF

HEK293T cells were transfected with mVWF cDNA. The colony with the highest amount of mVWF was selected, expanded, and compared to HUVEC. When comparing the supernatant of HUVEC and HEK293T, there is more VWF secreted by the HEK293T versus HUVEC (figure 30a). When comparing the supernatant of the HUVEC and the HEK293T, the hVWF ELISA demonstrates higher hVWF in HUVEC versus HEK293T; however, there is still hVWF detected in the HEK293T (figure 30b).

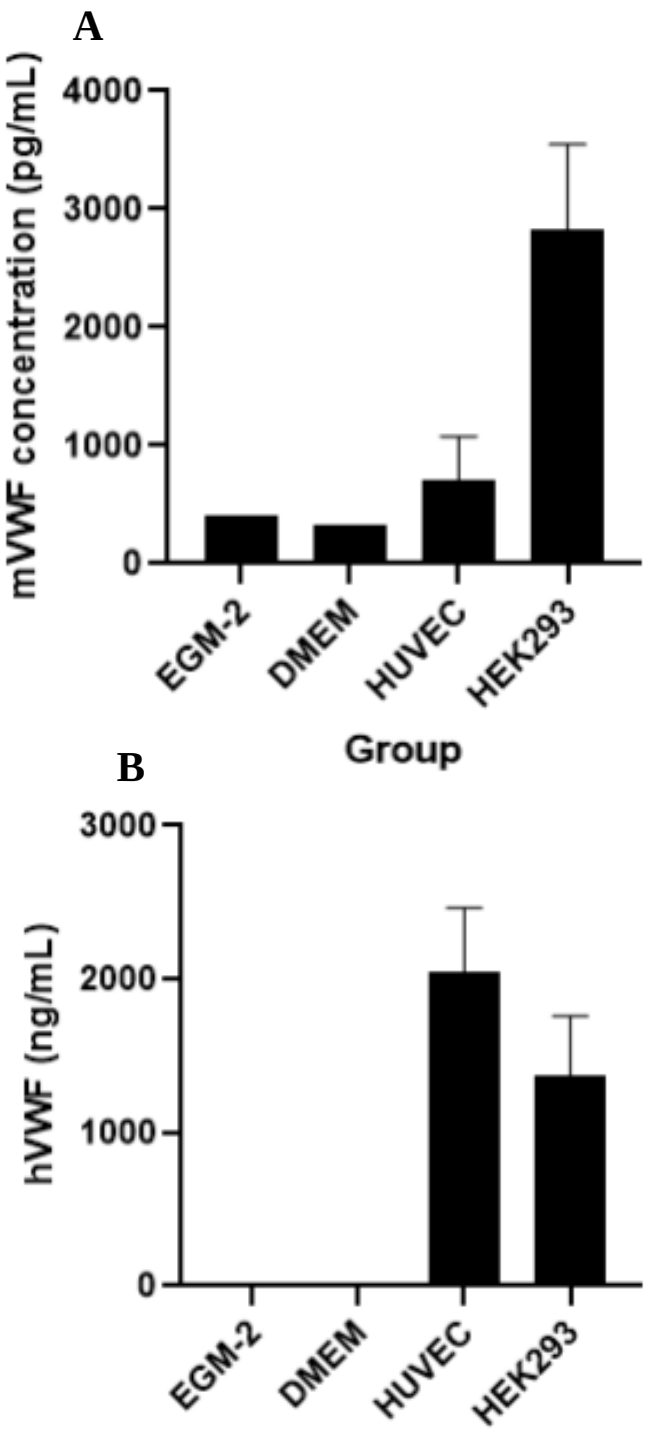

Figure 30. HEK293T cells were transfected with mVWF plasmid and VWF-producing colonies were selected. One colony (O) was plated and grown until 80% confluent and lysates and supernatant were collected. ELISA was performed on samples to determine VWF concentration. This caption represents mVWF (pg/mL) (A) and hVWF (ng/mL) (B) of HUVEC versus mVWF-transfected HEK293T supernatant samples and culture media only groups.

Chapter 4: Discussion

Current research on VWF expression in endothelial cells is limited to human endothelial cells *in vitro* (Pan *et al.,* 2016; Yamamoto *et al.,* 1998). These studies cannot always be an adequate representation of *in vivo* conditions in mice. Of these studies, VWF expression is only investigated in up to 24 hours time scale days (Kamalzare *et al.,* 2019; Takahashi *et al*, 2015; Hwang *et al*, 2010); however, novel treatments such as siRNA targeting VWF work on the scale of several days (Kamalzare *et al.,* 2019; Takahashi *et al*, 2015; Hwang *et al*, 2010). There is currently no research linking treatments and experiments of longer time scales with VWF expression.

Specifically, media was changed at 48 hours to mimic the media change that occurs during siRNA transfection to remove residual VWF. VWF is then measured 24 hours after the media change when transfecting cells, therefore the sane was applied here. To ensure VWF was removed after the media change, and to investigate the change in VWF expression between the media change and final 24-hour collection, samples were collected 30 minutes and 6 hours after the media change.

With VWF being a promising target to hemostatic pathologies such as thrombosis and VWD due to its role in these diseases (Xiang & Hwa, 2016) it is necessary to study *in vitro* VWF expressing models to be used to study these diseases. Specifically, due to VWFs role in disease, siRNA is a method to target VWF for knockdown that can be investigated as a possible treatment. With siRNA working on a larger time scale, I aimed to investigate VWF expression in human and mouse endothelial cells at time points relevant to siRNA transfection.

HUVECs were chosen as the human endothelial cell line that mouse cell lines are compared to because they are widely used to study VWF expression (Lenting *et al*., 2012).

LSEC was chosen due to the high expression of FVIII RNA and moderate expression of VWF in the liver sinusoids (Pan *et al.,* 2016). LMEC and iMAEC were chosen due to the high expression of VWF RNA in lung tissue and aorta (Pan *et al.,* 2016; Yamamoto *et al.,* 1998; Uhlén *et al.,* 2010; the protein atlas).

When investigating VWF protein expression, the results of the ELISA of untreated endothelial cells demonstrate that the expression pattern of the LSEC and iMAEC may be similar to the pattern of HUVEC. However, the increase in VWF at 24 hours demonstrated in the LSEC and iMAEC is not demonstrated for the HUVEC. A possible reason for this may be a decrease in cells that are secreting VWF due to the natural progression of cells into the decline phase which could result from different growth rates between cell lines. The difference between the LMEC and other cell supernatant samples could be due to different secretion and/or growth rates of the cells.

When examining the VWF RNA expression, both LSEC and iMAEC had an overall upregulation of VWF for both PMA and thrombin-treated cells; While LSEC and HUVEC had similar expression patterns with PMA-treated cells being upregulated at earlier time points and no upregulation seen at later time points or for thrombin-treated cells.

Immunofluorescence images demonstrate a slightly different VWF distribution between the mouse and human endothelial cells. VWF visualized in the HUVECS followed the typical cobblestone structure with VWF being secreted in Weibel-Palade bodies and being fairly evenly distributed throughout the cell; However, the mouse endothelial cells all have more of an elongated shape as seen through the VWF expression with the majority of VWF being seen closer to the center of the cells. There are also no visible Weibel-Palade bodies. This suggests that there may be slight difference in the morphology between human and mouse endothelial

cells. This also may be a result of physical cell stress including scraping of the cell monolayer or changes in ion concentrations in cell culture media (Thoumine *et al.*, 1995).

While supernatant from HEK293T cells transfected with mVWF was detected on the mVWF ELISA, it was also detected on the hVWF ELISA. It is possible that there may be a conserved portion of the sequence that allows for the detection by both human and mouse antibodies.

When comparing the results of all experiments, it seems that LSEC may be the most similar in terms of VWF expression to HUVECs; although it is not a perfect comparison. The differences between VWF expression between time points in each cell line can help narrow down the ideal timepoints for siRNA experiments. The highest VWF expression that is consistently seen between treatments, cell lines and protein vs RNA experiments is the 48h timepoint, however this is before changing media. After changing media, there does not seem to be a large increase in VWF between the 30 minute and 24 hours for HUVEC and iMAEC, but there is an increase for LSEC and LMEC. Since there is more detectable VWF for LSEC and LMEC at 24 hours, they may be more suitable for siRNA treatments, as the samples are also collected 24 hours after the media change. Alternatively, HUVEC and iMAEC may be cultured for a greater length of time after the media change to investigate peak VWF expression. siRNA transfection can be performed with a sample collection at 24 hours versus a longer incubation after media change to assess whether the longer incubation affects knockdown. That may help determine whether a human cell line with a similar secretion pattern to LSEC/LMEC should be chosen or if HUVECs/iMAECs are the better choice.

4.1 Limitations and future directions

Although HUVECs are the most commonly used cell line to study VWF, there may be other cell lines that may better represent pathologic conditions. Unlike umbilical vein cells, a variety of vascular endothelial cells that typically are affected by thrombosis in humans may be considered as an extra human cell line in the future. However, it is not guaranteed that the VWF expression in such cells will be as high as the expression in HUVECs. Depending on the expression levels of VWF, the use of other cell lines may or may not be ideal for VWF studies specifically. Using alternative cell lines would also allow for the direct comparison of mouse and human cell lines of the same tissue type.

The mouse aortic cell line used was chosen for high VWF expression in the heart, however they are immortalized which might not compare well to primary cell lines due to the rapid, uncontrolled growth that could results in differences in secretion contents and physiology.

These results, in conjunction with research on chosen siRNA vector, may be used to find the ideal timepoints and experimental design for siRNA transfection to knockdown VWF.

HEK293T cells are resistant to the selection media used, producing a transient cell line. In the future, HEK293T cells can be transfected using a plasmid containing resistance to a different antibiotic or a cell line not resistant to the selection media, such as HEK293 can be used to create a stable cell line. Additionally, cells that are not transfected with the VWF gene can be used as a control to demonstrate the non-transfected cells do not produce VWF.

4.2 Conclusions

While VWF may be a good target for the treatment of hematologic diseases such as thrombosis through siRNA, there are no current studies investigating VWF in endothelial cells at time points relevant to siRNA transfection. There are no studies investigating VWF expression in

mouse endothelial cells in culture. This study characterized the expression of VWF protein and RNA in untreated and stimulated HUVECS, LSEC, LMEC and iMAEC over a longer time course using ELISA, IF and qRT-PCR. These findings demonstrate varying VWF expression patterns between all the investigated cell lines. The changes in VWF expression over time can be used design experiments for siRNA transfection based on the cell line.

5. Supplementary Figures

A		0h	48h	30 min	6h	24h
Control	LSEC	331.6261	839.019	266.8034	249.3733	4481.658
	LMEC	481.234	858.5759	1316.978	1075.011	11659.9
	iMAEC	927.8384	1529.118	579.4784	893.8967	20739.89
	HUVEC	27927.2	59023.13	2491.612	1127.415	58.037
PMA	LSEC	331.6261	478.4495	127.3641	313.0142	5233.621
	LMEC	481.234	853.0614	334.5178	1032.383	17708.16

	iMAEC	927.8384	1290.245	732.521	755.7767	19606.03
	HUVEC	27927.2	76043.69	646.5345	9599.663	1603.813
	LSEC	331.6261	120.7243	145.6677	268.1603	3947.52
	LMEC	481.234	473.409	496.9769	689.5947	18315.61
	iMAEC	927.8384	1739.464	997.9849	795.6924	19493.55
Thrombin	HUVEC	27927.2	96884.76	1379.328	6723.88	1883.811

B		0h	48h	30 min	6h	24h
	LSEC	312.3313	620.4035	587.5147	405.4313	363.6756
	LMEC	215.5504	264.7984	362.1881	608.8507	235.6928
	iMAEC	892.3218	909.9243	1222.706	1237.171	1050.445
Control	HUVEC	572.1185	1409.014	886.1418	735.817	579.0278
	LSEC	312.3313	307.4414	191.5275	120.6055	252.2809
	LMEC	215.5504	140.0239	312.8821	265.7072	89.08187
	iMAEC	892.3218	498.2296	476.8782	375.8517	393.0442
PMA	HUVEC	572.1185	425.2393	1543.37	359.174	745.589
	LSEC	312.3313	340.9496	213.7694	114.25	226.3313
	LMEC	215.5504	170.3002	236.446	228.1802	132.8396
	iMAEC	892.3218	650.1187	609.3212	363.4325	357.8782
Thrombin	HUVEC	572.1185	8679.532	1097.897	1294.813	540.8958

Table S1. Comparison of VWF protein expression of untreated, PMA-treated, and thrombin-treated HUVEC, LSEC, LMEC and iMAEC supernatant (A) and lysates (B).

A	48h (ΔCT)	30 min (ΔCT)	6h (ΔCT)	24h (ΔCT)
LSEC	17.059	11.866	13.223	12.572
LMEC	18.975	19.991	18.522	17.050
iMAEC	19.730	18.846	18.138	16.179

HUVEC	22.617	1.0169	0.6459	0.387

B		Fold change (2^-(ΔΔCT)			
		48h	30 min	6h	24h
	LSEC	60230.410	22711.140	10.372	146.400
	LMEC	4.785	2.157	0.556	1.658
	iMAEC	2.840	1.055	0.742	1.143
PMA	HUVEC	3.560E+08	1.603	1.285	0.623
	LSEC	0.765	0.500	0.258	0.097
	LMEC	13166667.000	12258621.000	11109376.000	0.911
	iMAEC	1.022	0.601	0.234	0.222
Thrombin	HUVEC	147777.200	0.0003	6.110E-05	0.0001

Table S2. Comparison of relative VWF RNA expression of untreated LSEC, LMEC, iMAEC and HUVEC (A) and fold change between PMA-treated and thrombin-treated HUVEC, LSEC, LMEC and iMAEC (B). n=3

6. References

Adams, R. L., & Bird, R. J. (2009). Review article: Coagulation cascade and therapeutics update: Relevance to nephrology. Part 1: Overview of coagulation, thrombophilias and history of anticoagulants. *Nephrology, 14*(5), 462-470. doi:10.1111/j.1440-1797.2009.01128.x

Babich, V., Meli, A., Knipe, L., Dempster, J. E., Skehel, P., Hannah, M. J., & Carter, T. (2008). Selective release of molecules from Weibel-Palade bodies during a lingering kiss. *Blood*, *111*(11), 5282–5290. https://doi.org/10.1182/blood-2007-09-113746

Brill, A., Fuchs, T. A., Chauhan, A. K., Yang, J. J., De Meyer, S. F., Köllnberger, M., . . .Wagner, D. D. (2011). Von Willebrand factor–mediated platelet adhesion is critical for deep vein thrombosis in mouse models. *Blood*, *117*(4), 1400-1407. doi:10.1182/blood-2010-05-287623

Campioni, M., Legendre, P., Loubiere, C., Lunghi, B., Pinotti, M., Christophe, O. D., Lenting, P. J., Denis, C. V., Bernardi, F., & Casari, C. (2021). In vivo modulation of a dominant-negative variant in mouse models of von Willebrand disease type 2A. *Journal of thrombosis and haemostasis : JTH*, *19*(1), 139–146. https://doi.org/10.1111/jth.15131

Castaman, G., Goodeve, A., Eikenboom, J., & European Group on von Willebrand Disease (2013). Principles of care for the diagnosis and treatment of von Willebrand disease. *Haematologica*, *98*(5), 667–674. https://doi.org/10.3324/haematol.2012.077263

Chery J. (2016). RNA therapeutics: RNAi and antisense mechanisms and clinical applications. *Postdoc journal : a journal of postdoctoral research and postdoctoral affairs*, *4*(7), 35–50. https://doi.org/10.14304/surya.jpr.v4n7.5

Christopherson, P. A., Haberichter, S. L., Flood, V. H., Perry, C. L., Sadler, B. E., Bellissimo, D. B., Di Paola, J., Montgomery, R. R., & Zimmerman Program Investigators (2022). Molecular pathogenesis and heterogeneity in type 3 VWD families in U.S. Zimmerman program. *Journal of thrombosis and haemostasis : JTH*, *20*(7), 1576–1588. https://doi.org/10.1111/jth.15713

Crawley, J. T., & Scully, M. A. (2013). Thrombotic thrombocytopenic purpura: basic pathophysiology and therapeutic strategies. *Hematology. American Society of Hematology. Education Program*, *2013*, 292–299. https://doi.org/10.1182/asheducation-2013.1.292

Davie, E. W., Fujikawa, K., & Kisiel, W. (1991). The coagulation cascade: initiation, maintenance, and regulation. *Biochemistry*, *30*(43), 10363–10370. https://doi.org/10.1021/bi00107a001

de Maat, S., Clark, C. C., Barendrecht, A. D., Smits, S., van Kleef, N. D., El Otmani, H., Waning, M., van Moorsel, M., Szardenings, M., Delaroque, N., Vercruysse, K., Urbanus, R. T., Sebastian, S., Lenting, P. J., Hagemeyer, C. E., Renné, T., Vanhoorelbeke, K., Tersteeg, C., & Maas, C. (2022). Microlyse: a thrombolytic agent that targets VWF for clearance of microvascular thrombosis. *Blood*, *139*(4), 597–607. https://doi.org/10.1182/blood.2021011776

De Meyer, S. F., De Maeyer, B., Deckmyn, H., & Vanhoorelbeke, K. (2009). Von Willebrand factor: drug and drug target. *Cardiovascular & hematological disorders drug targets*, *9*(1), 9–20. https://doi.org/10.2174/187152909787581327

DiGiandomenico, S., Christopherson, P. A., Haberichter, S. L., Abshire, T. C., Montgomery, R. R., Flood, V. H., & Zimmerman Program Investigators (2021). Laboratory variability in the diagnosis of type 2 VWD variants. *Journal of thrombosis and haemostasis : JTH*, *19*(1), 131–138. https://doi.org/10.1111/jth.15129

Edvardsen, M. S., Hindberg, K., Hansen, E., Morelli, V. M., Ueland, T., Aukrust, P., . . . Hansen, J. (2021). Plasma levels of von Willebrand factor and future risk of incident venous

thromboembolism. *Blood Advances*, *5*(1), 224-232. doi:10.1182/bloodadvances.2020003135

Furie, B., & Furie, B. C. (2008). Mechanisms of thrombus formation. *The New England journal of medicine*, *359*(9), 938–949. https://doi.org/10.1056/NEJMra0801082

Goodeve, A., Eikenboom, J., Castaman, G., Rodeghiero, F., Federici, A. B., Batlle, J., Meyer, D., Mazurier, C., Goudemand, J., Schneppenheim, R., Budde, U., Ingerslev, J., Habart, D., Vorlova, Z., Holmberg, L., Lethagen, S., Pasi, J., Hill, F., Hashemi Soteh, M., Baronciani, L., … Peake, I. (2007). Phenotype and genotype of a cohort of families historically diagnosed with type 1 von Willebrand disease in the European study, Molecular and Clinical Markers for the Diagnosis and Management of Type 1 von Willebrand Disease (MCMDM-1VWD). *Blood*, *109*(1), 112–121. https://doi.org/10.1182/blood-2006-05-020784

Harter, K., Levine, M., & Henderson, S. (2015). Anticoagulation Drug Therapy: A Review. *Western Journal of Emergency Medicine*, *16*(1), 11-17. doi:10.5811/westjem.2014.12.22933

Hassan, M. I., Saxena, A., & Ahmad, F. (2012). Structure and function of von Willebrand factor. Blood Coagulation & Fibrinolysis, 23(1), 11-22. doi:10.1097/mbc.0b013e32834cb35d

Hurwitz, A., Massone, R., & Lopez, B. L. (2017). Acquired Bleeding Disorders. *Hematology/oncology clinics of North America*, *31*(6), 1123–1145. https://doi.org/10.1016/j.hoc.2017.08.012

Hwang, G.-W., Tobita, M., Takahashi, T., Kuge, S., Kita, K., & Naganuma, A. (2010). Sirna-mediated AMPK.ALPHA.1 subunit gene PRKAA1 silencing enhances methylmercury toxicity in HEK293 cells. *The Journal of Toxicological Sciences*, *35*(4), 601–604. https://doi.org/10.2131/jts.35.601

Jackson, S. P. (2011). Arterial thrombosis--insidious, unpredictable and deadly. *Nature medicine*, *17*(11), 1423–1436. https://doi.org/10.1038/nm.2515

Jilma-Stohlawetz, P., Gilbert, J. C., Gorczyca, M. E., Knöbl, P., & Jilma, B. (2011). A dose ranging phase I/II trial of the von Willebrand factor inhibiting aptamer ARC1779 in patients with congenital thrombotic thrombocytopenic purpura. *Thrombosis and haemostasis*, *106*(3), 539–547. https://doi.org/10.1160/TH11-02-0069

Kamalzare, S., Noormohammadi, Z., Rahimi, P., Atyabi, F., Irani, S., Tekie, F., & Mottaghitalab, F. (2019). Carboxymethyl dextran-trimethyl chitosan coated superparamagnetic iron oxide nanoparticles: An effective siRNA delivery system for HIV-1 Nef. *Journal of cellular physiology*, *234*(11), 20554–20565. https://doi.org/10.1002/jcp.28655

Kher, G., Trehan, S., & Misra, A. (2011). Antisense Oligonucleotides and RNA Interference. *Challenges in Delivery of Therapeutic Genomics and Proteomics*, 325–386. https://doi.org/10.1016/B978-0-12-384964-9.00007-4

Kim, J. H., Lim, K., & Gwak, H. S. (2017). New Anticoagulants for the Prevention and Treatment of Venous Thromboembolism. *Biomolecules & Therapeutics*, *25*(5), 461-470. doi:10.4062/biomolther.2016.271

Kleinschnitz, C., Meyer, S. F., Schwarz, T., Austinat, M., Vanhoorelbeke, K., Nieswandt, B., Stoll, G. (2009). Deficiency of von Willebrand factor protects mice from ischemic stroke. *Blood*, *113*(15), 3600-3603. doi:10.1182/blood-2008-09-180695

Lenting, P. J., Casari, C., Christophe, O. D., & Denis, C. V. (2012). von Willebrand factor: The old, the new and the unknown. *Journal of Thrombosis and Haemostasis*, *10*(12), 2428–2437. https://doi.org/10.1111/jth.12008

Lipinski, B., Pretorius, E., Oberholzer, H. M., & van der Spuy, W. J. (2012). Interaction of fibrin with red blood cells: the role of iron. *Ultrastructural pathology*, *36*(2), 79–84. https://doi.org/10.3109/01913123.2011.627491

Longstaff, C., & Kolev, K. (2015). Basic mechanisms and regulation of fibrinolysis. *Journal of thrombosis and haemostasis : JTH*, *13 Suppl 1*, S98–S105. https://doi.org/10.1111/jth.12935

López, J. A., & Chen, J. (2009). Pathophysiology of venous thrombosis. *Thrombosis research*, *123 Suppl 4*, S30–S34. https://doi.org/10.1016/S0049-3848(09)70140-9

Lopes da Silva, M., & Cutler, D. F. (2016). von Willebrand factor multimerization and the polarity of secretory pathways in endothelial cells. *Blood*, *128*(2), 277–285. https://doi.org/10.1182/blood-2015-10-677054

Mackman, N. (2008). Triggers, targets and treatments for thrombosis. *Nature*, *451*(7181), 914–918. https://doi.org/10.1038/nature06797

Meiring, M., Allers, W., & Le Roux, E. (2016). Tissue factor: A potent stimulator of Von Willebrand factor synthesis by human umbilical vein endothelial cells. *International journal of medical sciences*, *13*(10), 759–764. https://doi.org/10.7150/ijms.15688

Monroe, D. M., & Hoffman, M. (2006). What does it take to make the perfect clot?. *Arteriosclerosis, thrombosis, and vascular biology*, *26*(1), 41–48. https://doi.org/10.1161/01.ATV.0000193624.28251.83

Moriya J. (2019). Critical roles of inflammation in atherosclerosis. *Journal of cardiology*, *73*(1), 22–27. https://doi.org/10.1016/j.jjcc.2018.05.010

Nathwani A. C. (2019). Gene therapy for hemophilia. *Hematology. American Society of Hematology. Education Program*, *2019*(1), 1–8. https://doi.org/10.1182/hematology.2019000007

Newby, D. E., Wright, R. A., Labinjoh, C., Ludlam, C. A., Fox, K. A., Boon, N. A., & Webb, D. J. (1999). Endothelial dysfunction, impaired endogenous fibrinolysis, and cigarette smoking: a mechanism for arterial thrombosis and myocardial infarction. *Circulation*, *99*(11), 1411–1415. https://doi.org/10.1161/01.cir.99.11.1411

Nieswandt, B., Pleines, I., & Bender, M. (2011). Platelet adhesion and activation mechanisms in arterial thrombosis and ischaemic stroke. *Journal of thrombosis and haemostasis : JTH*, *9 Suppl 1*, 92–104. https://doi.org/10.1111/j.1538-7836.2011.04361.x

Nightingale, T., & Cutler, D. (2013). The secretion of von W Willebrand factor from endothelial cells; an increasingly complicated story. Journal of Thrombosis and Haemostasis, 11(S1), 192-201. doi:10.1111/jth.12225

Oklu R. (2017). Thrombosis. *Cardiovascular diagnosis and therapy*, *7*(Suppl 3), S131–S133. https://doi.org/10.21037/cdt.2017.11.08

Osborn, M. F., & Khvorova, A. (2018). Improving siRNA Delivery In Vivo Through Lipid Conjugation. *Nucleic acid therapeutics*, *28*(3), 128–136. https://doi.org/10.1089/nat.2018.0725

Pan, J., Dinh, T. T., Rajaraman, A., Lee, M., Scholz, A., Czupalla, C. J., Kiefel, H., Zhu, L., Xia, L., Morser, J., Jiang, H., Santambrogio, L., & Butcher, E. C. (2016). Patterns of expression of factor VIII and von Willebrand factor by endothelial cell subsets in vivo. *Blood*, *128*(1), 104–109. https://doi.org/10.1182/blood-2015-12-684688

Peyvandi, F., Kouides, P., Turecek, P. L., Dow, E., & Berntorp, E. (2019). Evolution of replacement therapy for von Willebrand disease: From plasma fraction to recombinant von Willebrand factor. *Blood reviews*, *38*, 100572. https://doi.org/10.1016/j.blre.2019.04.001

Sanders, Y. V., Eikenboom, J., De Wee, E. M., Van der Bom, J. G., Cnossen, M. H., Degenaar-Dujardin, M. E., . . . Leebeek, F. W. (2013). Reduced prevalence of arterial thrombosis in von Willebrand disease. *Journal of Thrombosis and Haemostasis, 11*(5), 845-854. doi:10.1111/jth.12194

Schroeder, A., Levins, C. G., Cortez, C., Langer, R., & Anderson, D. G. (2010). Lipid-based nanotherapeutics for siRNA delivery. *Journal of internal medicine*, *267*(1), 9–21. https://doi.org/10.1111/j.1365-2796.2009.02189.x

Springer, T. A. (2014). Von Willebrand factor, Jedi Knight of the bloodstream. Blood, 124(9), 1412-1425. doi:10.1182/blood-2014-05-378638

Sukumar, S., Lämmle, B., & Cataland, S. R. (2021). Thrombotic Thrombocytopenic Purpura: Pathophysiology, Diagnosis, and Management. *Journal of clinical medicine*, *10*(3), 536. https://doi.org/10.3390/jcm10030536

Szederjesi, A., Baronciani, L., Budde, U., Castaman, G., Colpani, P., Lawrie, A. S., Liu, Y., Montgomery, R., Peyvandi, F., Schneppenheim, R., Patzke, J., & Bodó, I. (2020). Comparison of von Willebrand factor platelet-binding activity assays: ELISA overreads type 2B with loss of HMW multimers. *Journal of thrombosis and hemostasis JTH*, *18*(10), 2513–2523. https://doi.org/10.1111/jth.14971

Takahashi, T., Kim, M.-S., Hwang, G.-W., Kuge, S., & Naganuma, A. (2015). Knockdown of acyl-COA thioesterase 9 gene expression by Sirna confers resistance to arsenite in HEK293 cells. *Fundamental Toxicological Sciences*, *2*(6), 245–247. https://doi.org/10.2131/fts.2.245

The human protein atlas. The Human Protein Atlas. (n.d.). Retrieved September 4, 2022, from https://www.proteinatlas.org/

Thoumine, O., Ziegler, T., Girard, P. R., & Nerem, R. M. (1995). Elongation of confluent endothelial cells in culture: the importance of fields of force in the associated alterations of their cytoskeletal structure. *Experimental cell research*, *219*(2), 427–441. https://doi.org/10.1006/excr.1995.1249

Turner, N. A., Nolasco, L., Ruggeri, Z. M., & Moake, J. L. (2009). Endothelial cell ADAMTS-13 and VWF: production, release, and VWF string cleavage. *Blood*, *114*(24), 5102–5111. https://doi.org/10.1182/blood-2009-07-231597

Turpie, A. G., & Esmon, C. (2011). Venous and arterial thrombosis--pathogenesis and the rationale for anticoagulation. *Thrombosis and haemostasis*, *105*(4), 586–596. https://doi.org/10.1160/TH10-10-0683

Uhlen, M., Oksvold, P., Fagerberg, L., Lundberg, E., Jonasson, K., Forsberg, M., Zwahlen, M., Kampf, C., Wester, K., Hober, S., Wernerus, H., Björling, L., & Ponten, F. (2010). Towards a knowledge-based Human Protein Atlas. *Nature biotechnology*, *28*(12), 1248–1250. https://doi.org/10.1038/nbt1210-1248

Westein, E., Flierl, U., Hagemeyer, C.E. and Peter, K. (2013), Targeted Drug Delivery in Atherosclerosis and Thrombosis. *Drug Dev. Res*., 74: 460-471. https://doi.org/10.1002/ddr.21103

Wolberg, A. S., Aleman, M. M., Leiderman, K., & Machlus, K. R. (2012). Procoagulant activity in hemostasis and thrombosis: Virchow's triad revisited. *Anesthesia and analgesia*, *114*(2), 275–285. https://doi.org/10.1213/ANE.0b013e31823a088c

Xiang, Y., & Hwa, J. (2016). Regulation of VWF expression, and secretion in health and disease. *Current opinion in hematology*, *23*(3), 288–293. https://doi.org/10.1097/MOH.0000000000000230

Yamamoto, K., de Waard, V., Fearns, C., & Loskutoff, D. J. (1998). Tissue Distribution and Regulation of Murine von Willebrand Factor Gene Expression In Vivo. *Blood*, *92*(8), 2791–2801. https://doi.org/10.1182/blood.V92.8.2791

Zhou, Y. F., Eng, E. T., Nishida, N., Lu, C., Walz, T., & Springer, T. A. (2011). A pH-regulated dimeric bouquet in the structure of von Willebrand factor. *The EMBO journal*, *30*(19), 4098–4111. https://doi.org/10.1038/emboj.2011.297